

A Generalized Approach to Indeterminacy in Linear Rational Expectations Models*

Francesco Bianchi Giovanni Nicolò
Duke University Federal Reserve Board
CEPR and NBER

10th September 2020

Abstract

We propose a novel approach to deal with the problem of indeterminacy in Linear Rational Expectations models. The method consists of augmenting the original state space with a set of auxiliary exogenous equations to provide the adequate number of explosive roots in presence of indeterminacy. The solution in this expanded state space, if it exists, is always determinate, and is identical to the indeterminate solution of the original model. The proposed approach accommodates determinacy and any degree of indeterminacy, and it can be implemented even when the boundaries of the determinacy region are unknown. Thus, the researcher can estimate the model using standard software packages without restricting the estimates to the determinacy region. We combine our solution method with a novel hybrid Metropolis-Hastings algorithm to estimate the New-Keynesian model with rational bubbles by Galí (forthcoming) over the period 1982:Q4-2007:Q3. We find that the data support the presence of two degrees of indeterminacy, implying that the central bank was not reacting strongly enough to the bubble component.

JEL classification: C19, C51, C62, C63.

Keywords: Indeterminacy, General Equilibrium, Solution method, Bayesian methods.

*The views expressed in this paper are those of the authors and do not reflect the views of the Federal Reserve Board or the Federal Reserve System. We thank Jonas Arias, Jess Benhabib, Roger Farmer, Francois Geerolf, Frank Schorfheide, and all participants at UCLA seminars, NBER Multiple Equilibria and Financial Crises Conference, CEPR-IMFS New Methods for Macroeconomic Modeling, Model Comparison and Policy Analysis Conference, Federal Reserve Bank of St. Louis, Society of Economic Dynamics, 12th Dynare Conference, 2017 NBER-NSF conference on Bayesian Inference in Econometrics and Statistics. Correspondence: Francesco Bianchi, Duke University, Department of Economics. Email: francesco.bianchi@duke.edu. Giovanni Nicolò, Board of Governors of the Federal Reserve System. Email: giovanni.nicolo@frb.gov.

1 Introduction

Sunspot shocks and multiple equilibria have been at the center of economic thinking at least since the seminal work of Cass and Shell (1983), Farmer and Guo (1994), and Farmer and Guo (1995). The zero lower bound has brought renovated interest to the problem of indeterminacy (Aruoba et al., 2018). Furthermore, in many of the Linear Rational Expectation (LRE) models used to study the properties of the macroeconomy the possibility of multiple equilibria arises for some parameter values, but not for others. This paper proposes a novel approach to solve LRE models that easily accommodates both the case of determinacy and indeterminacy. As a result, the proposed methodology can be used to easily solve and estimate a LRE model that could potentially be characterized by multiplicity of equilibria. Our approach is implementable even when the analytic conditions for determinacy or the degrees of indeterminacy are unknown. Importantly, the proposed method can be easily implemented to study indeterminacy in standard software packages, such as Dynare (Adjemian et al., 2011) and Sims' (2001) code Gensys.

To understand how our approach works, it is useful to recall the conditions for determinacy as stated by Blanchard and Kahn (1980). Indeterminacy arises when the parameter values are such that the number of explosive roots is smaller than the number of non-predetermined variables. The key idea of our method is to augment the original model by appending additional autoregressive processes that can be used to provide the missing explosive roots. The innovations of these exogenous processes are assumed to be linear combinations of a subset of the forecast errors associated with the expectational variables of the model and a newly defined vector of sunspot shocks. When the Blanchard-Kahn condition for determinacy is satisfied, all the roots of the auxiliary autoregressive processes are assumed to be within the unit circle and the auxiliary process is irrelevant for the dynamics of the model. In this case, the law of motion for the endogenous variables is equivalent to the solution obtained using standard solution algorithms (King and Watson, 1998; Klein, 2000; Sims, 2001). When the model is indeterminate, the appropriate number of appended autoregressive processes is assumed to be explosive. For example, if there are two degrees of indeterminacy, two of the auxiliary processes are assumed to be explosive. The solution that we obtain for the endogenous variables is equivalent to the one obtained with the methodology of Lubik and Schorfheide (2003) or Farmer et al. (2015).

Our methodology simplifies the common approach used to deal with indeterminacy. The common procedure requires the researcher to solve the model differently depending on the area of the parameter space that is being studied. Under indeterminacy, existing methods require to either construct the solution ex-post following the seminal contribution of Lubik and Schorfheide (2003) or rewrite the model based on the existing degree of indeterminacy (Farmer et al., 2015). In itself, this is not an insurmountable task, but it implies that the researcher cannot simply use

standard solution methods or software packages. What is more, if the researcher is interested in a structural estimation of the model, she would need to write the estimation codes and not just the solution codes. Our proposed method only requires the researcher to augment the original system of equations to reflect the maximum degree of indeterminacy and can therefore be used with standard solution approaches and estimation packages such as Dynare.

Our method can also be combined with sophisticated Bayesian techniques to facilitate the transition between the determinacy and indeterminacy regions of the parameter space. One possibility would be to adopt the sequential Monte Carlo algorithm of Herbst and Schorfheide (2015b) as in Hirose et al. (2020) and Ettmeier and Kriwoluzky (2020). In this paper, we instead propose an hybrid Metropolis-Hastings algorithm that builds on a specific example developed in An and Schorfheide (2007) following Giordani et al. (2010). The algorithm combines the standard Metropolis-Hastings random walk algorithm with a Markov Chain Monte Carlo (MCMC) algorithm in which the proposal distribution is based on a mixture of normals centered on the different posterior modes. This algorithm guarantees that the chain quickly moves to the region of the parameter space with the highest posterior and allows to visit local peaks with more frequency.

We combine our solution method with the proposed hybrid Metropolis-Hastings algorithm to estimate the small-scale New-Keynesian (NK) model of Galí (forthcoming) using Bayesian techniques on U.S. data over the period 1982:Q4 until 2007:Q3. Galí's model extends a conventional NK model to allow for the existence of rational bubbles. An interesting aspect of the model is that it displays up to two degrees of indeterminacy for realistic parameter values. We find that the data support the version of the model with two degrees of indeterminacy, implying that the central bank was not reacting strongly enough to the bubble component. Importantly, we show that the combination of our method with the hybrid algorithm ensures a significantly faster transition to the region of the parameter space with the best model fit relative to a standard Metropolis-Hastings random walk algorithm. Furthermore, in Section 6, we re-consider the NK model of Lubik and Schorfheide (2004) to show that the proposed algorithm also ensures a more efficient exploration of the parameter space when regions of the parameters characterized by different degrees of indeterminacy present a more similar fit by increasing significantly the frequency with which the different regions are visited.

Our work is related to the vast literature that studies the role of indeterminacy in explaining the evolution of the macroeconomy. Prominent examples in the monetary policy literature include the work of Clarida et al. (2000) and Kerr and King (1996), that study the possibility of multiple equilibria as a result of violations of the Taylor Principle in NK models. Applying the methods developed in Lubik and Schorfheide (2003) to the canonical NK model, Lubik and Schorfheide (2004) test for indeterminacy in U.S. monetary policy. Using a calibrated small-scale model,

Coibon and Gorodnichenko (2011) find that the reduction of the target inflation rate in the United States also played a key role in explaining the Great Moderation, and Arias et al. (forthcoming) support this finding in the context of a medium-scale model *à la* Christiano et al. (2005). More recently, Aruoba et al. (2018) study inflation dynamics at the Zero Lower Bound (ZLB) and during an exit from the ZLB.

The paper closest to ours is Farmer et al. (2015). The main difference between the two approaches is that our method accommodates the case of both determinacy and indeterminacy while considering the same augmented system of equations. Instead, the method proposed by Farmer et al. (2015) requires rewriting the model based on the existing degree of indeterminacy.

With respect to Lubik and Schorfheide (2003), our theoretical results show the characterization of the full set of indeterminate equilibria is equivalent between the two methods. Our novel approach provides a unified methodology to study determinacy and indeterminacy of different degrees.¹ Lubik and Schorfheide (2004) propose a baseline solution that minimizes the distance between the impulse responses of the model under indeterminacy and determinacy evaluated at the boundary of the region of determinacy. Given the equivalence between our methods, their baseline solution can be mapped into our representation. However, as explained in Subsection 2.2, our method naturally suggests a baseline solution that sets the correlations of the fundamental disturbances with the sunspot shocks to zero. Such identification can be equivalently thought as an assumption that fundamental shocks do not have a *contemporaneous* impact on the variables whose sunspot shocks are considered as drivers of the economy. This identification strategy is reminiscent of the zero restrictions often used in the Structural VAR (SVAR) literature. Importantly, the baseline solution is just meant to provide an intuitive and simple-to-implement benchmark and does not impose a constraint on a researcher who wants to consider alternative solutions.

The remainder of the paper is organized as follows. Section 2 builds the intuition by using a univariate example in the spirit of Lubik and Schorfheide (2004) and discusses how to construct the baseline solution in our method. In Section 3, we present the methodology and show that the augmented representation of the LRE model delivers solutions which under determinacy are equivalent to those obtained using standard solution algorithms, and under indeterminacy to those obtained using the methodology provided by Lubik and Schorfheide (2003, 2004) and Farmer et al. (2015). In Section 4, we describe the hybrid algorithm proposed to facilitate the estimation of models with different degrees of indeterminacy. In Section 5, we apply our method and the proposed hybrid algorithm to estimate the NK model with rational bubbles of Galí (forthcoming). Section 6 discusses the advantages of using the proposed hybrid algorithm when estimating models, such as Lubik and Schorfheide (2004), in which the fit across regions

¹Ascari et al. (2019) allow for temporarily unstable paths, while we require all solutions to be stationary, in line with previous contributions in the literature.

of determinacy is similar. We present our conclusions in Section 7.

2 Building the intuition

In this section, we consider a univariate example in the spirit of Lubik and Schorfheide (2004) to provide the intuition behind our solution method and to explain how to construct the associated baseline solution.

2.1 A useful example

Consider a classical monetary model characterized by the Fisher equation, $i_t = E_t(\pi_{t+1}) + r_t$, and the simple Taylor rule, $i_t = \phi_\pi \pi_t$, where i_t denotes the nominal interest rate, π_t represents the inflation rate, and $\phi_\pi > 0$ is a parameter controlling the response of the nominal interest to inflation. We assume that the real interest rate, r_t , is given and described by a mean-zero Gaussian i.i.d. shock.² To properly specify the model, we also define the one-step ahead forecast error associated with the expectational variable, π_t , as $\eta_t \equiv \pi_t - E_{t-1}(\pi_t)$.

Combining the Fisher equation and the simple Taylor rule, we obtain the univariate model

$$E_t(\pi_{t+1}) = \phi_\pi \pi_t - r_t. \quad (1)$$

Any solution to (1) satisfies

$$\pi_t = \phi_\pi \pi_{t-1} - r_{t-1} + \eta_t. \quad (2)$$

First, we consider the case $\phi_\pi > 1$. Solving (2) forward and recalling the assumptions on r_t , it is clear that this case is associated with the determinate solution

$$\left\{ \pi_t = \frac{1}{\phi_\pi} r_t, \eta_t = \frac{1}{\phi_\pi} r_t \right\}. \quad (3)$$

The strong response of the monetary authority to changes in inflation ($\phi_\pi > 1$) guarantees that inflation is pinned down as a function of the exogenous real interest rate r_t . From a technical perspective, when $\phi_\pi > 1$ the Blanchard-Kahn condition for uniqueness of a solution is satisfied: The number of explosive roots matches the number of expectational variables, that in this univariate case is one.

The second case corresponds to $\phi_\pi \leq 1$. The solution corresponds to *any* process that takes the form in (2). Such solution also holds under determinacy, but in that case the central bank's

²In the classical monetary model, the real interest rate results from the equilibrium in labor and goods market, and it depends on the technology shocks. We are considering an exogenous process for the technology shocks, and therefore we take the process for the real interest rate as given.

behavior induces restrictions on the expectation error η_t as a function of the exogenous shock, r_t . Instead, when the monetary authority does not respond aggressively enough to changes in inflation ($\phi_\pi \leq 1$), there are multiple solutions for the inflation rate, π_t , each indexed by the expectations that the representative agent holds about future inflation, η_t . Equivalently, the solution to the univariate model is indeterminate: The Blanchard-Kahn solution is not satisfied as there is no explosive root to match the number of expectational variables.³ Finally, the fundamental shock r_t has a contemporaneous effect on inflation only to the extent that it affects the expectational error η_t .

The simple model considered here can be solved pencil and paper. However, when considering richer models with multiple endogenous variables, indeterminacy represents a challenge from a methodological and computational perspective. Standard software packages such as Dynare do not allow for indeterminacy. Of course, a researcher could in principle code an estimation algorithm herself, following the methods outlined in Lubik and Schorfheide (2004). However, this approach requires a substantial amount of time and technical skills. The researcher would need to write a code that not only finds the solution, but also implements the estimation algorithm. Hence, the result is that in practice most of the papers simply rule out the possibility of indeterminacy, even if the model at hand could in principle allow for such a feature.

To alleviate these issues, our methodology consists of augmenting the original state space of the model by appending an auxiliary process which could be either stable or unstable

$$\begin{cases} E_t(\pi_{t+1}) = \phi_\pi \pi_t - r_t, \\ \omega_t = \left(\frac{1}{\alpha}\right) \omega_{t-1} - \nu_t + \eta_t, \end{cases} \quad (4)$$

where ω_t is an independent autoregressive process, $\alpha \in [0, 2]$ and ν_t is a newly defined mean-zero sunspot shock with standard deviation σ_ν and correlation $\rho_{\nu r}$.

Table 1 summarizes the intuition behind our approach.⁴ When the original LRE model in (1) is determinate ($\phi_\pi > 1$), the auxiliary process must be stationary ($1/\alpha < 1$), so that the augmented representation in (4) satisfies the Blanchard-Kahn condition.⁵ In this case, the method of Sims (2001) delivers the same solution for the endogenous variable π_t as in equation (3). Importantly, ω_t represents a separate block and does not impact the endogenous variable π_t .

Considering the case of indeterminacy ($\phi_\pi \leq 1$), the original model has one expectational variable, but no unstable root, thus violating the Blanchard-Kahn condition. By appending an explosive autoregressive process ($1/\alpha > 1$), the solution in this expanded state space is determinate as

³To ensure boundedness, the indeterminate solution requires the forecast error, η_t , to be any covariance-stationary martingale difference process.

⁴We refer the reader to Appendix D for detailed suggestions on the practical implementation of our method.

⁵The choice of parametrizing the auxiliary process with $1/\alpha$ instead of α induces a positive correlation between ϕ_π and α that facilitates the implementation of our method when estimating a model.

Determinacy $\phi_\pi > 1$ in original model (1)	Unstable roots	B-K condition in augmented model (4)	Solution
$\frac{1}{\alpha} < 1$	1	Satisfied	$\begin{cases} \pi_t = \frac{1}{\phi_\pi} r_t, & \eta_t = \frac{1}{\phi_\pi} r_t \\ \omega_t = \alpha \omega_{t-1} - \nu_t + \eta_t \end{cases}$
$\frac{1}{\alpha} > 1$	2	Not satisfied	-
Indeterminacy $\phi_\pi \leq 1$ in original model (1)			
$\frac{1}{\alpha} < 1$	0	Not satisfied	-
$\frac{1}{\alpha} > 1$	1	Satisfied	$\begin{cases} \pi_t = \phi_\pi \pi_{t-1} - r_{t-1} + \nu_t \\ \eta_t = \nu_t, & \omega_t = 0 \end{cases}$

Table 1: Blanchard-Kahn condition in the augmented representation.

The table reports the regions of the parameter space for which the Blanchard-Kahn condition in the augmented representation is satisfied, even when the original model is indeterminate.

the Blanchard-Kahn condition is satisfied for the augmented system, even if not for the original model. In particular, the solution for the endogenous variable π_t corresponds to the one in (2) resulting from the methodology of Lubik and Schorfheide (2003) or Farmer et al. (2015). Moreover, stability imposes conditions such that ω_t is always equal to zero at any time t , thus requiring to impose ω_0 equal to zero and $\eta_t = \nu_t$. Importantly, even in this case ($\phi_\pi \leq 1$), the solution for the endogenous variable does not depend on the appended autoregressive process. Under this scenario, shocks to the real interest rate have a contemporaneous effect on inflation only through their effect on the sunspot shock, as we explain in more detail below.

Finally, in both cases, the auxiliary process ω_t constitutes a separate block that is not mapped into an observable variable. The process ω_t only serves the purpose of providing the necessary explosive roots under indeterminacy and creating a mapping from the sunspot shock to the expectational error. Therefore, the law of motion of the endogenous variables is invariant with respect to the adoption of our method to solve the model.

2.2 Baseline solution

Our augmented representation parametrizes the continuum of equilibria under indeterminacy by introducing the standard deviation of the sunspot shock included in the auxiliary processes, σ_ν , and its correlation, $\rho_{\nu r}$, with the fundamental shock. In this section, we propose a baseline solution that arises naturally in the context of our solution method.

Lubik and Schorfheide (2004) propose a baseline solution that minimizes the distance between the impulse response functions of the model under indeterminacy and determinacy evaluated at the boundary of the region of determinacy. In Section 3, our theoretical results show the equivalence between our methods and therefore the possibility of mapping their baseline solution

into our representation. However, it is not always immediate to construct the baseline solution proposed by Lubik and Schorfheide (2004), given that the boundaries of the determinacy region are often unknown.

In our approach, the baseline solution restricts to zero the correlation $\rho_{\nu r}$, implying *no contemporaneous* impact of the fundamental shock, r_t , on inflation, π_t . In Table 1, the indeterminate solution is such that the expectational variable, π_t , is predetermined and its contemporaneous deviations from its steady state are only due to the sunspot shock, ν_t . In other words, the fundamental shock r_t can affect π_t only if it affects the sunspot shock ν_t . Thus, it seems natural to choose as baseline solution the one associated with no correlation between the sunspot shock and the fundamental shock, r_t . Such identification strategy equivalently implies that the fundamental shock does not have a contemporaneous impact on the inflation rate and is therefore reminiscent of the zero restrictions often used in the SVAR literature. The baseline solution represents a useful benchmark, but it is not restrictive: All alternative solutions can be obtained by allowing the correlation between the fundamental and sunspot shock to be different from zero.

3 Methodology

We now present the main contribution of the paper generalizing the intuition provided above to a multivariate model with potentially multiple degrees of indeterminacy. Given the general class of LRE models described in Sims (2001), this paper proposes an augmented representation which embeds the solution for the model under both determinacy and indeterminacy. In particular, the augmented representation of the LRE model delivers solutions which under determinacy are equivalent to those obtained using standard solution algorithms, and under indeterminacy to those obtained using the methodology provided by Lubik and Schorfheide (2003, 2004) or Farmer et al. (2015).

Consider the following LRE model

$$\Gamma_0(\theta)X_t = \Gamma_1(\theta)X_{t-1} + \Psi(\theta)\varepsilon_t + \Pi(\theta)\eta_t, \quad (5)$$

where $X_t \in R^k$ is a vector of endogenous variables, $\varepsilon_t \in R^\ell$ is a vector of exogenous shocks, $\eta_t \in R^p$ collects the p one-step ahead forecast errors for the expectational variables of the system and $\theta \equiv \text{vec}(\Gamma_0, \Gamma_1, \Psi, \Omega_{\varepsilon\varepsilon})' \in \Theta$ is a vector of structural parameters of the model as well as the covariance matrix of the exogenous shocks. The matrices Γ_0 and Γ_1 are of dimension $k \times k$, possibly singular, and the matrices Ψ and Π are of dimension $k \times \ell$ and $k \times p$, respectively. Also, we assume $E_{t-1}(\varepsilon_t) = E_{t-1}(\eta_t) = 0$. We also define the $\ell \times \ell$ matrix $\Omega_{\varepsilon\varepsilon} \equiv E_{t-1}(\varepsilon_t\varepsilon_t')$ to represent the covariance matrix of the exogenous shocks.

Consider a model whose maximum degree of indeterminacy is denoted by m .⁶ The proposed methodology appends to the original LRE model in (5) the following system of m equations

$$\omega_t = \Phi\omega_{t-1} + \nu_t - \eta_{f,t}, \quad \Phi \equiv \begin{bmatrix} \alpha_1^{-1} & & \mathbf{0} \\ & \ddots & \\ \mathbf{0} & & \alpha_m^{-1} \end{bmatrix} \quad (6)$$

where the vector $\eta_{f,t}$ is a subset of the endogenous shocks and the vectors $\{\omega_t, \nu_t, \eta_{f,t}\}$ are of dimension $m \times 1$. The equations in (6) are autoregressive processes whose innovations are linear combinations of a vector of newly defined sunspot shocks, ν_t , and a subset of forecast errors, $\eta_{f,t}$, where $E_{t-1}(\nu_t) = E_{t-1}(\eta_{f,t}) = 0$. As we will show below, the choice of which expectational errors to include in (6) does not affect the solution.

The intuition behind the proposed methodology works as in the example considered in the previous section. Let $m^*(\theta)$ denote the actual degree of indeterminacy associated with the parameter vector θ . Under indeterminacy the Blanchard-Kahn condition for the original LRE model in (5) is not satisfied. Given that the system is characterized by $m^*(\theta)$ degrees of indeterminacy, it is necessary to introduce $m^*(\theta)$ explosive roots to solve the model using standard solution algorithms. In this case, $m^*(\theta)$ of the diagonal elements of the matrix Φ are assumed to be outside the unit circle (in absolute value), and the augmented representation is therefore determinate because the Blanchard-Kahn condition is now satisfied. On the other hand, under determinacy the (absolute value of the) diagonal elements of the matrix Φ are assumed to be all inside the unit circle, as the number of explosive roots of the original LRE model in (5) already equals the number of expectational variables in the model ($m^*(\theta) = 0$). Also, in this case the augmented representation is determinate due to the stability of the appended auxiliary processes. Importantly, as shown for the univariate example in Section 2, the block structure of the proposed methodology guarantees that the autoregressive process, ω_t , never affects the solution for the endogenous variables, X_t .

Denoting the newly defined vector of endogenous variables $\hat{X}_t \equiv (X_t, \omega_t)'$ and the newly defined vector of exogenous shocks $\hat{\varepsilon}_t \equiv (\varepsilon_t, \nu_t)'$, the system in (5) and (6) can be written as

$$\hat{\Gamma}_0 \hat{X}_t = \hat{\Gamma}_1 \hat{X}_{t-1} + \hat{\Psi} \hat{\varepsilon}_t + \hat{\Pi} \eta_t, \quad (7)$$

⁶Denoting by n the minimum number of unstable roots of a LRE model and p the number of one-step ahead forecast errors, the maximum degrees of indeterminacy are defined as $m \equiv p - n$. When the minimum number of unstable roots of a model is unknown, then m coincides with number of expectational variables p . This represents the maximum degree of indeterminacy in any model with p expectational variables.

where

$$\hat{\Gamma}_0 \equiv \begin{bmatrix} \Gamma_0(\theta) & \mathbf{0} \\ \mathbf{0} & \mathbf{I} \end{bmatrix}, \quad \hat{\Gamma}_1 \equiv \begin{bmatrix} \Gamma_1(\theta) & \mathbf{0} \\ \mathbf{0} & \Phi \end{bmatrix}, \quad \hat{\Psi} \equiv \begin{bmatrix} \Psi(\theta) & \mathbf{0} \\ \mathbf{0} & \mathbf{I} \end{bmatrix}, \quad \hat{\Pi} \equiv \begin{bmatrix} \Pi_n(\theta) & \Pi_f(\theta) \\ 0 & -\mathbf{I} \end{bmatrix},$$

and it is without loss of generality that we partition the matrix Π in (5) as $\Pi = [\Pi_n \quad \Pi_f]$, where the matrices Π_n and Π_f are respectively of dimension $k \times (p - m)$ and $k \times m$.⁷ Indeed, a unique mapping exists between the alternative representations that can be considered using our augmented representation. In the online Appendix, we use an analytic example to show that the alternative representations are equivalent up to a transformation of the correlations between the exogenous shocks and the forecast error included in the auxiliary process.

We now show that the augmented representation of the LRE model delivers solutions which in the determinate region of the parameter space, Θ^D , are equivalent to those obtained using standard solution algorithms, and in the indeterminate region, Θ^I , to those obtained using the methodology provided by Lubik and Schorfheide (2003, 2004) and Farmer et al. (2015).⁸ This theoretical result is crucial for the application of our methodology to the New-Keynesian (NK) model with rational bubbles of Galí (forthcoming) in Section 5.

3.1 Determinate equilibrium and equivalent characterizations

The characterization of a determinate equilibrium of the original system in (5) is a vector $\theta^D \in \Theta^D$. The characterization of the solution under determinacy using the proposed augmented representation is parametrized by the set of parameters θ^{BN} that combines the vector $\theta^D \in \Theta^D$ with the set of additional parameters $\theta_1 \in \Theta_1$, where the vector $\theta_1 \equiv \text{vec}(\Omega_{\nu\nu}, \Omega_{\nu\varepsilon})'$ collects the elements of the covariance matrix of the sunspot shocks, $\Omega_{\nu\nu}$, and the parameters of the covariances, $\Omega_{\nu\varepsilon}$, between the sunspot shock ν_t and the exogenous shocks ε_t .

Theorem 1 *Let θ^D and θ^{BN} be two parametrizations of a determinate equilibrium of the model*

$$\Gamma_0 X_t = \Gamma_1 X_{t-1} + \Psi \varepsilon_t + \Pi \eta_t.$$

For the BN equilibrium parametrized by θ^{BN} , the solution for the endogenous variables, X_t , is equivalent to the solution parameterized by θ^D and is independent of the additional parameters θ_1 .

⁷Suppose that $\Pi_{k \times 3} \equiv \begin{bmatrix} \Pi_1 & \Pi_2 & \Pi_3 \\ k \times 1 & k \times 1 & k \times 1 \end{bmatrix}$. The proposed augmented representation would therefore allow for the following three possible alternatives, $\hat{\Pi}_1 \equiv \begin{bmatrix} \Pi_1 & \Pi_2 & \Pi_3 \\ 0 & 0 & -1 \end{bmatrix}$, $\hat{\Pi}_2 \equiv \begin{bmatrix} \Pi_1 & \Pi_2 & \Pi_3 \\ 0 & -1 & 0 \end{bmatrix}$ and $\hat{\Pi}_3 \equiv \begin{bmatrix} \Pi_1 & \Pi_2 & \Pi_3 \\ -1 & 0 & 0 \end{bmatrix}$.

⁸In order to simplify the exposition, when analyzing the case of indeterminacy we assume, without loss of generality, $m^*(\theta) = m$. As it will become clear, the case of $m^*(\theta) < m$ is a special case of what we present below.

Proof. See Appendix A. ■

The intuition for this theorem can be understood by considering the determinate solution to the univariate example reported in Table 1. First, the endogenous variable, π_t , is only a function of the exogenous shock r_t , and *not* of the newly defined sunspot shock, ν_t . Similarly, the endogenous variables, X_t , of the original LRE model in (5) do not respond to sunspot shocks either as expected under determinacy. Second, the univariate example shows that under determinacy the appended system of equations constitutes a separate block which does not affect the dynamics of the endogenous variable, π_t . Similarly, the solution for the endogenous variables, X_t , constitutes a separate block relative to the auxiliary variables, ω_t , and is therefore independent of the additional parameters θ_1 .

3.2 Indeterminate equilibria and equivalent characterizations

The indeterminate equilibria found using the methodology of Lubik and Schorfheide (2003) are parametrized by two sets of parameters. The first set is defined by $\theta^I \in \Theta^I$. In addition, given that the system is indeterminate, Lubik and Schorfheide (2003) append additional m equations,

$$\begin{matrix} \widetilde{M} & \varepsilon_t & + & M_\zeta & \zeta_t & = & V_2' & \eta_t \\ m \times \ell & \ell \times 1 & & m \times m & m \times 1 & & m \times p & p \times 1 \end{matrix} \quad (8)$$

Given the normalization $M_\zeta = I$ chosen by Lubik and Schorfheide (2004), the second set corresponds to $\theta_2 \in \Theta_2$, where $\theta_2 \equiv \text{vec}(\Omega_{\zeta\zeta}, \widetilde{M})'$. Equation (8) introduces $m \times (m+1)/2$ parameters associated with the covariance matrix of the sunspot shocks, $\Omega_{\zeta\zeta}$, and additional $m \times \ell$ parameters of the matrix \widetilde{M} that is related to the covariances between η_t and ε_t . The characterization of a Lubik-Schorfheide equilibrium is a vector $\theta^{LS} \in \Theta^{LS}$, where Θ^{LS} is defined as

$$\Theta^{LS} \equiv \{\Theta^I, \Theta_2\}.$$

Similarly, the full characterization of the solutions under indeterminacy using the proposed augmented representation is parametrized by the set of parameters $\theta^I \in \Theta^I$ common between the two methodologies, and the set of additional parameters $\theta_1 \in \Theta_1$. Using our approach, we also introduce $m \times (m+1)/2$ parameters associated with the covariance matrix of the sunspot shocks, $\Omega_{\nu\nu}$, and $m \times \ell$ parameters of the covariances, $\Omega_{\nu\varepsilon}$, between the sunspot shocks ν_t and the exogenous shocks ε_t . A Bianchi-Nicolò equilibrium is characterized by a parameter vector $\theta^{BN} \in \Theta^{BN}$, where Θ^{BN} is defined as

$$\Theta^{BN} \equiv \{\Theta^I, \Theta_1\}.$$

The following theorem establishes the equivalence between the characterizations of indeterminate equilibria obtained by using the methodology in Lubik and Schorfheide (2003) and the proposed augmented representation.

Theorem 2 *Let θ^{LS} and θ^{BN} be two alternative parametrizations of an indeterminate equilibrium of the model*

$$\Gamma_0 X_t = \Gamma_1 X_{t-1} + \Psi \varepsilon_t + \Pi \eta_t.$$

For every BN equilibrium, parametrized by θ^{BN} , there exists a unique matrix \widetilde{M} and a unique matrix $\Omega_{\zeta\zeta}$ such that $\theta_2 = \text{vec}(\Omega_{\zeta\zeta}, \widetilde{M})'$, and $\{\theta_1, \theta_2\} \in \Theta^{LS}$ defines an equivalent LS equilibrium. Conversely, for every LS equilibrium, parametrized by θ^{LS} , there is a unique matrix $\Omega_{\nu\nu}$ and a unique covariance matrix $\Omega_{\nu\varepsilon}$ such that $\theta_3 = \text{vec}(\Omega_{\nu\nu}, \Omega_{\nu\varepsilon})'$, and $\{\theta_1, \theta_3\} \in \Theta^{BN}$ defines an equivalent BN equilibrium.

Proof. See Appendix A. ■

In the paper Farmer et al. (2015), the authors also show that their characterization of indeterminate equilibria is equivalent to Lubik and Schorfheide (2003). Therefore, the following corollary holds.

Corollary 1 *Given a parametrization θ^{BN} of a BN indeterminate equilibrium, there exists a unique mapping into the parametrization of an indeterminate equilibrium for Farmer et al. (2015), and vice-versa.*

In a multivariate model, the construction of the baseline solution relies on the key insight of the univariate model in Subsection 2.2. Under indeterminacy, the expectational variables whose forecast error is included in the explosive auxiliary processes *always* become predetermined and their contemporaneous deviations from their steady state are *only* a function of their respective sunspot shock. Therefore, our method naturally suggests a baseline solution that sets the correlations of the sunspot shocks with fundamental disturbances, $\Omega_{\nu\varepsilon}$, to zero. Such identification assumption implies that fundamental shocks do not have a contemporaneous impact on those expectational variables, in line with the zero restrictions often used in the SVAR literature. At the same time, the identifying assumption implies that sunspot shocks are not in any way related to fundamental disturbances, a natural starting point for an economic analysis. Finally, under such baseline solution, the choice of *which* forecast errors, $\eta_{f,t}$, to include in the auxiliary processes delivers different economic assumptions.⁹ However, the choice of the *ordering* of the forecast errors *within* the vector, $\eta_{f,t}$, is irrelevant to determine the impact of fundamental shocks on the expectational variables.

⁹Appendix D provides a more detailed and practical discussion on the choice of the prior distributions for the correlations between the sunspot shocks and fundamental disturbances.

4 Inference

To facilitate inference in a model that allows for different degrees of indeterminacy, several papers, such as Hirose et al. (2020) and Ettmeier and Kriwoluzky (2020), adopted the sequential Monte Carlo algorithm of Herbst and Schorfheide (2015b). Such algorithm could be combined with our method to estimate models characterized by indeterminacy. In this section, we propose an alternative approach that pairs our method with an Hybrid Metropolis-Hastings algorithm.

As discussed by Lubik and Schorfheide (2004), a researcher that estimates a model with different degrees of indeterminacy often faces the challenging situation in which the posterior can present jumps along the boundaries of the determinacy and indeterminacy regions. Furthermore, these models often present local peaks in the posterior distribution with the result that a Metropolis-Hastings random walk algorithm might end up gravitating around one of these local peaks. To alleviate these problems, we propose an hybrid algorithm that combines the standard Metropolis-Hastings random walk algorithm with a MCMC algorithm in which the proposal distribution is based on a mixture of normals centered on the different posterior modes. The idea of using an hybrid algorithm to improve the efficiency of the standard Metropolis-Hastings random walk algorithm is extensively discussed in Herbst and Schorfheide (2015a) and Giordani et al. (2010). The algorithm proposed here builds on one specific example discussed in An and Schorfheide (2007). In what follows, we describe the key steps.

1. Using different starting values, apply a numerical optimization procedure to search for modes $\tilde{\theta}_{(j)}$, $j = 1, \dots, J$ of the posterior density. When the model allows for different degrees of indeterminacy, the search can be conditioned on determinacy or indeterminacy. This guarantees that each of the regions has a, possibly local, posterior mode.
2. For each mode, compute the inverse of the Hessian, denoted by $\tilde{\Sigma}_{(j)}$, $j = 1, \dots, J$.
3. Let $q_j(\theta)$ be the density of a multivariate distribution obtained mixing two normals, both with mean $\tilde{\theta}_{(j)}$, but different covariance matrices $c_j^s \tilde{\Sigma}_{(j)}$ and $c_j^l \tilde{\Sigma}_{(j)}$, with $c_j^s < c_j^l$. Let z^l be the probability of drawing from the normal with large variance:

$$q_j(\theta) = z^l N\left(\tilde{\theta}_{(j)}, c_j^l \tilde{\Sigma}_{(j)}\right) + (1 - z^l) N\left(\tilde{\theta}_{(j)}, c_j^s \tilde{\Sigma}_{(j)}\right).$$

4. Let π_j , $j = 1, \dots, J$ be a set of probabilities and define $q(\theta)$ as:

$$q(\theta) = \sum_{j=1}^J \pi_j q_j(\theta).$$

5. Choose a starting value $\theta^{(0)}$ for instance by generating a draw from $q(\theta)$.

6. For $s = 1, \dots, nsim$, follow these steps:

(a) Make a draw ϑ from the following proposal distribution:

$$\begin{aligned}\tilde{q}(\vartheta|\theta^{(s-1)}) &= w^{RW} N\left(\theta^{(s-1)}, c^{RW} \tilde{\Sigma}_{(j)}\right) + (1 - w^{RW}) q(\theta) \\ &= w^{RW} N\left(\theta^{(s-1)}, c^{RW} \tilde{\Sigma}_{(j)}\right) \\ &\quad + (1 - w^{RW}) \left[z^l N\left(\tilde{\theta}_{(j)}, c_j^l \tilde{\Sigma}_{(j)}\right) + (1 - z^l) N\left(\tilde{\theta}_{(j)}, c_j^s \tilde{\Sigma}_{(j)}\right) \right]\end{aligned}$$

where w^{RW} is a number between 0 and 1 denoting the probability of using the standard random walk proposal distribution.

(b) Accept the jump from $\theta^{(s-1)}$ to ϑ ($\theta^{(s)} = \vartheta$) with probability $\min\left\{1, r_j\left(\theta^{(s-1)}, \vartheta|Y\right)\right\}$, otherwise reject the proposed draw and set $\theta^{(s)} = \theta^{(s-1)}$, where

$$r_j\left(\theta^{(s-1)}, \vartheta|Y\right) = \frac{\mathcal{L}(\vartheta|Y) p(\vartheta) / \tilde{q}(\vartheta|\theta^{(s-1)})}{\mathcal{L}(\theta^{(s-1)}|Y) p(\theta^{(s-1)}) / \tilde{q}(\theta^{(s-1)}|\vartheta)}$$

Note that point 6 collapses to a standard Metropolis-Hastings algorithm if $w^{RW} = 1$, while it becomes similar to the hybrid MCMC algorithm proposed by An and Schorfheide (2007) to deal with a multimodal posterior if $w^{RW} = 0$. The use of the mixture of normals facilitates the jump between areas of the parameter space that gravitate around different peaks of the posterior. The advantage of allowing for the standard random walk proposal distribution is to allow the algorithm to explore the parameter space around these peaks in an efficient way. In other words, the standard random walk algorithm has generally a higher acceptance rate and does not face the risk of getting stuck on a value for which the ratio between the posterior and the proposal distribution is particularly high.

Convergence. A researcher should appropriately conduct convergence diagnostics by verifying the occurrence of either of the following two circumstances. First, a multimodal distribution could arise because the log-likelihood is highly discontinuous between the various regions. In this case, the algorithm could jump towards the region where the peak of the posterior lies, without having spent a significant time there. In other words, convergence has not occurred yet. We therefore recommend the researcher to analyze the draws of the parameter(s) α_i which have been accepted during the MCMC algorithm. By inspecting the behavior of the auxiliary parameter(s) α_i , a researcher can detect if the algorithm reached convergence or not. If the convergence has not occurred yet, the researcher should repeat the estimation exercise increasing the number of draws and making sure that the parameter(s) α_i stabilizes on one region of the parameter space. Our main application in Section 5 is an example of this case and we show that the hybrid

algorithm guarantees a faster convergence than the standard Metropolis-Hastings to the region of the parameter space with the best fit to the data.

Second, a multimodal distribution could arise because the fit of the model at the global peak is only marginally better than that at the local peak in a different region of indeterminacy. In this case, the parameter(s) α_i would repeatedly transition between the two areas of the parameter space and could be used to infer the probability attached to determinacy. An example of this second case is considered in Section 6 when we estimate the model in Lubik and Schorfheide (2004). In such instance, we show the advantage of the hybrid algorithm is to visit the different peaks of the posterior in the different regions with a substantially higher frequency relative to a random walk algorithm, allowing for a more efficient exploration of the parameter space and a faster convergence of the MCMC algorithm.

5 Monetary policy and asset bubbles

In this section, we implement the proposed methodology to estimate the small-scale NK model of Galí (forthcoming) using Bayesian techniques. The model extends a conventional NK model to allow for the existence of rational expectations equilibria with asset price bubbles. Interestingly, the model displays up to two degrees of indeterminacy for realistic parameter values.

We estimate the model using U.S. data over the period 1982:Q4 - 2007:Q3, and we consider the case that the U.S. monetary policy aimed at stabilizing the inflation rate and leaning against the bubble. We find that the strength of such responses was not enough to guarantee a stabilization of the U.S. economy and to avoid that unexpected changes in expectations could drive U.S. business cycles. In particular, we show that the model specification that provides the best fit to the data is characterized by two degrees of indeterminacy.

5.1 Model

Galí (forthcoming) extends a standard version of the NK model to allow, under certain conditions, the emergence of fluctuations driven by asset price bubbles in equilibrium. The model introduces overlapping generations of finitely-lived consumers to ensure that the transversality condition of any individual consumer is satisfied in equilibrium, even in the presence of a bubble that grows at the rate of interest. The model also assumes stochastic transitions to “retirement,” generating an equilibrium interest rate not exceeding the economy’s trend growth rate that is a necessary condition for the size of the bubble to remain bounded relative to the size of the economy.

The equations that describe the model are the following. First, equation (9) represents a dynamic IS curve

$$y_t = \Phi E_t(y_{t+1}) - \Psi [i_t - E_t(\pi_{t+1})] + \Theta q_t, \quad (9)$$

where the variables are expressed in deviations from a balanced growth path (henceforth BGP), and the parameters $\{\Phi, \Psi, \Theta\}$ are function of the structural parameters of the model.¹⁰ The term q_t denotes the size of an aggregate bubble in the economy (normalized by trend output) relative to its value along the BGP.

The aggregate bubble plays the role of demand shifter and is defined as

$$q_t = b_t + u_t^q, \quad (10)$$

where b_t denotes the aggregate value in period t of bubble assets that were already available for trade in period $t-1$, and u_t^q is the value of a new bubble at time t . We assume that u_t^q follows an exogenous autoregressive process of the form $u_t^q = \rho_q u_{t-1}^q + \varepsilon_t^q$, where $\varepsilon_t^q \stackrel{iid}{\sim} N(0, \sigma_q^2)$. Equation (11) defines the evolution of the value of the asset bubble q_t as

$$q_t = \Lambda \Gamma E_t (b_{t+1}) - q (i_t - E_t (\pi_{t+1})), \quad (11)$$

where $q \equiv \frac{\gamma(\beta - \Lambda \Gamma v)}{(1 - \beta \gamma)(1 - \Lambda \Gamma v \gamma)}$ represents the steady state bubble-to-output ratio, $\Lambda \equiv 1/(1 + r)$ is the steady state stochastic discount factor for one-period ahead payoffs derived from a portfolio of securities and $\Gamma \equiv (1 + g)$ is the gross rate of productivity growth. Equation (11) shows how “optimistic” expectations about the future value of the bubble lead to a higher price for the assets today. As shown in Galí (forthcoming), the existence of a BGP with positive asset bubbles requires that $\Lambda \Gamma v < \beta$. In addition, to guarantee that newly created bubbles are non-negative along the BGP, the model requires that $\Lambda \Gamma \geq 1$. Equivalently, these two conditions imply that there exists a continuum of bubbly BGPs indexed by a real interest rate in the range $\Gamma v / \beta - 1 < r \leq g$.

The model features a NK Phillips curve

$$\pi_t = \Lambda \Gamma v \gamma E_t (\pi_{t+1}) + \kappa y_t + u_t^s, \quad (12)$$

where $u_t^s = \rho_s u_{t-1}^s + \varepsilon_t^s$ and $\varepsilon_t^s \stackrel{iid}{\sim} N(0, \sigma_s^2)$.¹¹ Note that both the dynamic IS curve in (9) and the NK Phillips curve in (12) nest the standard NK model when the probability of death and retirement approach zero (i.e. $\{v, \gamma\} \rightarrow 1$), given that $\Lambda \Gamma = \beta$ along a balanced growth path

¹⁰The dynamic IS curve in (9) combines equations (30)–(34) in Galí (forthcoming) such that the parameters $\Phi \equiv \frac{\Lambda \Gamma v}{\beta} \in (0, 1]$, $\Psi \equiv \Upsilon \Phi \left(1 + \frac{v \gamma (1 - \Phi)}{\Phi (1 - \beta \gamma)}\right)$, $\Upsilon \equiv \frac{1 - \beta \gamma}{1 - \Lambda \Gamma v \gamma} \in (0, 1]$ and $\Theta \equiv \frac{(1 - \beta \gamma)(1 - v \gamma)}{\beta \gamma}$ are function of the following structural parameters: i) γ , the constant probability of each individual in the OLG model to survive to the next period; ii) v , the probability of each individual to be employed in the next period; iii) β , the discount factor of each individual; iv) $\Lambda \equiv 1/(1 + r)$, the steady state stochastic discount factor for one-period ahead payoffs derived from a portfolio of securities; v) $\Gamma \equiv (1 + g)$, the gross rate of productivity growth.

¹¹In particular, $k \equiv \frac{(1 - \theta)(1 - \Lambda \Gamma v \gamma \theta)}{\theta} \rho$, where θ represents the Calvo probability that a firm keeps its price unchanged in any given period and ρ is the elasticity of hours worked.

under the assumption of an infinitely-lived representative consumer with log utility.

Finally, the conduct of monetary policy follows an interest rate rule that features some inertia and aims not only at stabilizing inflation, but also at leaning against the bubble:

$$i_t = \rho_i i_{t-1} + (1 - \rho_i) (\phi_\pi \pi_t + \phi_q q_t) + \varepsilon_t^i, \quad (13)$$

where $\varepsilon_t^i \stackrel{iid}{\sim} N(0, \sigma_i^2)$. Note that, because of the absence of a trade-off between stabilization of inflation and output gap, the “divine coincidence” still holds in this modified version of the standard NK model, and the macroeconomic impact of bubble fluctuations mainly work through aggregate demand.

Equations (9)~(13) describe the equilibrium dynamics of the model economy around a given BGP. We define the vector of variables $X_t \equiv (y_t, \pi_t, b_t, i_t, q_t, E_t(y_{t+1}), E_t(\pi_{t+1}), E_t(b_{t+1}), u_t^q, u_t^s)'$, the vector of fundamental shocks, $\varepsilon_t \equiv (\varepsilon_t^q, \varepsilon_t^s, \varepsilon_t^i)'$, and the vector of non-fundamental errors, $\eta_t \equiv (\eta_{y,t}, \eta_{\pi,t}, \eta_{b,t})'$, where the rational expectation forecast errors are defined as $\eta_{x,t} \equiv x_t - E_{t-1}[x_t]$ and $x = \{y, \pi, b\}$.

As shown in Subsection 5.3 below, the model of Galí (forthcoming) is characterized by up to two degrees of indeterminacy. Therefore, the proposed methodology augments the model by appending two autoregressive processes

$$\omega_{j,t} = \alpha_j^{-1} \omega_{j,t-1} + \nu_{j,t} - \eta_{j,t}, \quad j = \{1, 2\}, \quad (14)$$

where $\{\eta_{1,t}, \eta_{2,t}\}$ could be any combination consisting of two of the three forecast errors defined by the vector $\eta_t \equiv (\eta_{y,t}, \eta_{\pi,t}, \eta_{b,t})'$. Hence, defining a new vector of endogenous variables $\hat{X}_t \equiv (X_t, \omega_{1,t}, \omega_{2,t})'$ and a newly defined vector of exogenous shocks as $\hat{\varepsilon}_t \equiv (\varepsilon_t, \nu_{1,t}, \nu_{2,t})'$, the system can then be written in canonical form.

5.2 Data and priors

We estimate the model to match U.S. data over the period 1982:Q4 until 2007:Q3. We consider three macroeconomic quarterly time series: the growth rate in real GDP, measured as the log change in real GDP, inflation, measured by the log change in the GDP deflator, and the Federal Funds rate. The measurement equations that relate the macroeconomic data to the endogenous variables are defined as

$$\begin{bmatrix} \Delta \log(GDP_t) \\ \Delta \log(P_t) \\ FFR_t \end{bmatrix} = \begin{bmatrix} g \\ \pi^* \\ r + \pi^* \end{bmatrix} + \begin{bmatrix} y_t - y_{t-1} \\ \pi_t \\ i_t \end{bmatrix}.$$

Table 2 reports the prior distributions for the parameters. We calibrate three parameters to guarantee identification. Following Galí (forthcoming), we calibrate the discount factor of each individual, β , to 0.998 and the probability of surviving to the next period, γ , to 0.996. As mentioned when studying equation (11) describing the evolution of the value of the asset bubble q_t , the model requires that the real interest rate, r , and the growth rate of output, g , satisfy $r \leq g$ to ensure that newly created bubbles along the BGP are non-negative. To ensure that this inequality holds for each draw of the Metropolis-Hastings algorithm, we express the real interest rate, r , as $r = \lambda_u g$, where $\lambda_u \in (0, 1]$ defines the ratio between the real interest rate and its upper bound, the rate of output growth. We then calibrate λ_u to 0.925 and set the prior for the quarterly growth rate of output, g , as a gamma distribution centered at 0.45. These assumptions imply an annualized growth rate of output of 1.8% and real interest rate of approximately 1.65% over the considered period.

As previously discussed, the existence of a BGP with positive asset bubbles requires that $v < \beta/\Lambda\Gamma$, where v is the probability that an individual remains “active” by supplying labor and managing the firm, as opposed to “retiring” with probability $(1 - v)$. Hence, we express such probability as $v = \lambda_l \beta/\Lambda\Gamma$, where $\lambda_l \in (0, 1)$. We then center the gamma prior distribution for the term $100(\lambda_l^{-1} - 1)$ such that the probability of remaining “active,” v , is 0.9973, therefore coinciding with the calibration in Galí (forthcoming). The resulting range of admissible BGPs is indexed by an (annualized) real interest rate $r \in (\Gamma v/\beta - 1, g] = (1.5\%, 1.8\%]$.

The prior for the slope of the NK Phillips Curve, κ , is set at 0.04, a value consistent with an average duration of individual prices of 4 quarters in this model. The parameter describing the response of the monetary authority to changes in inflation, ϕ_π , follows a gamma distribution with mean 1 and standard error 0.4. The response to deviations of the bubble relative to its value along the BGP, ϕ_q , follows a gamma distribution with mean 0.05 and standard error 0.02, corresponding to a region of the parameter space with up to two degrees of indeterminacy. Finally, the autoregressive parameter of the interest rate rule, ρ_i , follows a beta distribution with mean 0.5 and standard error 0.2.

The prior distribution of the supply and monetary policy shocks are inverse gamma centered at 0.3 with a standard deviation of 0.15. The inverse gamma prior for the shock associated with the creation of a new bubble, ε_t^q , is more agnostic and centered at 1 with standard deviation 0.5. Finally, when we estimate the model under indeterminacy, we specify uniform prior distributions for the standard deviations of the non-fundamental shocks $\{\sigma_{\nu_l}\}$ where $l = \{\pi, y, b\}$, and their correlations with both the exogenous shocks of the model $\{\varphi_{\nu_l, j}\}$ where $j = \{i, q, s\}$ and between them $\{\varphi_{\nu_{l_1}, \nu_{l_2}}\}$ where $\{l_1, l_2\} = \{\pi, y, b\}$. Importantly, to ensure that the covariance matrix is always positive definite, the joint prior for the covariance matrix is effectively truncated by rejecting the parameter draws that violate this condition.

	Posteriors		Density	Priors	
	Mean	90% prob. int.		Mean	Std. Dev.
$100(\lambda_l^{-1}-1)$	0.028	[0.019,0.038]	<i>Gamma</i>	0.04	0.01
κ	0.038	[0.030,0.047]	<i>Gamma</i>	0.04	0.005
g	0.48	[0.43,0.53]	<i>Gamma</i>	0.45	0.04
π^*	0.91	[0.47,1.48]	<i>Gamma</i>	0.9	0.30
ϕ_π	0.37	[0.18,0.65]	<i>Gamma</i>	1	0.40
ϕ_q	0.04	[0.02,0.09]	<i>Gamma</i>	0.05	0.02
ρ_i	0.49	[0.23,0.76]	<i>Beta</i>	0.50	0.20
σ_q	1.19	[0.58,2.19]	<i>Inv. Gam.</i>	1.00	0.50
σ_s	0.11	[0.09,0.14]	<i>Inv. Gam.</i>	0.30	0.15
σ_i	0.12	[0.10,0.15]	<i>Inv. Gam.</i>	0.30	0.15
ρ_q	0.76	[0.56,0.91]	<i>Beta</i>	0.70	0.10
ρ_s	0.87	[0.77,0.93]	<i>Beta</i>	0.70	0.10
σ_{ν_π}	0.29	[0.25,0.34]	$U[0, 10]$	5	2.89
σ_{ν_y}	0.70	[0.62,0.81]	$U[0, 10]$	5	2.89
$\varphi_{\nu_\pi,i}$	-0.60	[-0.77,-0.34]	$U[-1, 1]$	0	0.57
$\varphi_{\nu_\pi,q}$	0.23	[-0.25,0.60]	$U[-1, 1]$	0	0.57
$\varphi_{\nu_\pi,s}$	0.53	[0.34,0.67]	$U[-1, 1]$	0	0.57
$\varphi_{\nu_y,i}$	-0.40	[-0.69,-0.07]	$U[-1, 1]$	0	0.57
$\varphi_{\nu_y,q}$	0.05	[-0.43,0.54]	$U[-1, 1]$	0	0.57
$\varphi_{\nu_y,s}$	-0.54	[-0.70,-0.34]	$U[-1, 1]$	0	0.57
φ_{ν_π,ν_y}	0.22	[0.04,0.40]	$U[-1, 1]$	0	0.57

Table 2: Prior and posterior distributions of model parameters.

The table reports the prior and posterior distributions under two degrees of indeterminacy $\{\nu_\pi, \nu_y\}$.

5.3 Results

The hybrid algorithm and the best-fitting model specification. We estimate the model using the hybrid algorithm described in Section 4. Using different starting values and applying a numerical optimization procedure, we find the conditional posterior mode in each region of the parameter space: Determinacy, one degree of indeterminacy, and two degrees of indeterminacy. We then use those posterior modes to construct the proposal distribution as in step 6 of the hybrid algorithm. In what follows, we consider the specification in which the two auxiliary processes in (14) include the non-fundamental errors associated with inflation and output, $\{\eta_{1,t}, \eta_{2,t}\} = \{\eta_{\pi,t}, \eta_{y,t}\}$. When the algorithm draws a vector of structural parameters θ such that the model is indeterminate of degree 1, we set only α_1 to a value within the unit circle in a way that only the non-fundamental shock $\eta_{\pi,t}$ is redefined as fundamental. When the algorithm draws θ such that the model is indeterminate of degree 2, we set both α_1 and α_2 to a value within the unit circle

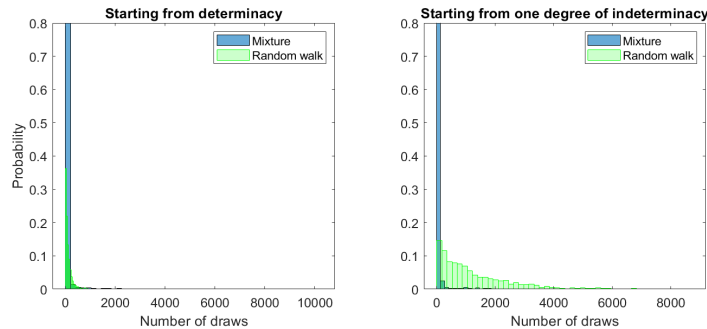


Figure 1: Distribution of number of draws necessary to cross to the indeterminacy-2 region.

The figure reports the distribution for the number of draws necessary to cross the determinacy and indeterminacy of degree 1 threshold for the first time when using two distinct algorithms to estimate the model of Galí (2018). Two cases are considered. In the first case (blue/dark colored bars), we use the hybrid algorithm ("Mixture") described in Section 4. In the second case (green/light colored bars), we use a standard Metropolis-Hastings random walk algorithm ("Random walk").

such that both non-fundamental shocks $\{\eta_{\pi,t}, \eta_{y,t}\}$ are redefined as fundamental. In Appendix B, we show that the estimation delivers the same posterior distributions of the model parameters regardless of which forecast errors we include in our representation.¹²

Starting the algorithm at values in each region of the parameter space, we find that the data favor the specification of the model with two degrees of indeterminacy. The algorithm quickly moves to that region of the parameter space and never leaves. This can be explained inspecting the log-posterior mode of the different regions of the parameters space: -30.93 with two degrees of indeterminacy, -44.94 with one degree of indeterminacy, and -119.66 with determinacy. These large differences could in principle represent a problem for traditional MCMC algorithms. In fact, the adoption of the hybrid algorithm ("Mixture") proposed in Section 4 considerably speeds up the transition to the region with two degrees of indeterminacy relative to a standard Metropolis-Hasting random walk algorithm ("Random walk").

To illustrate how the Mixture algorithm helps to ensure a more efficient convergence to the region of the parameter space with the highest posterior, we estimate the model using both algorithms. We simulate 2,000 chains by making an initial draw around the posterior mode of either the region of determinacy or indeterminacy of degree 1. For each iteration, we count the number of draws necessary for the parameters to cross the two-degree indeterminacy threshold for the first time. If the transition has not occurred after 100,000 iterations, we stop and record this upper bound. Using both the Mixture and the Random walk algorithms, Figure 1 reports the histogram

¹²As explained in Section 3, the posterior distributions of the model parameters are equivalent up to a transformation of the correlations between the exogenous shocks and the sunspot disturbances considered in each specification.

Starting value	Algorithm	Mean	Median	5%	95%
Determinacy	Mixture	89	17	2	165
	Random walk	118	72	6	390
Indeterminacy-1	Mixture	90	21	2	201
	Random walk	1294	874	48	3822

Table 3: Summary statistics for the distribution of number of draws necessary to cross to the indeterminacy-2 region.

The table reports summary statistics for the distribution of the number of draws necessary to cross to the region with two degrees of indeterminacy for different starting values and using both the hybrid algorithm ("Mixture") and the standard Metropolis-Hastings random walk algorithm ("Random walk").

of the number of draws necessary to jump to the region of two degrees of indeterminacy when starting from the region of determinacy (left panel) or indeterminacy of degree 1 (right panel). Table 3 reports the corresponding summary statistics of the plotted distributions.

Both algorithms eventually move to the region of the parameter space that contains the global peak. Once they reach such region, the chains do not jump back to explore the other regions where the fit of the model at the local peaks is substantially worse. However, the Mixture algorithm ensures a considerably faster switch to the region of the parameter space with the global peak.¹³ For starting values in the region of one-degree indeterminacy, the median number of draws necessary for the Mixture algorithm is nearly 15 times smaller than the corresponding statistic for the Random walk algorithm. Moreover, when we experimented with alternative versions of the model that imposed restrictions on some model parameters, we found that, for the traditional algorithm, the parameters had *not* crossed the two-degree indeterminacy threshold even after 100,000 iterations.

The convergence to one region of the parameter space can be easily checked tracking the behavior of the auxiliary parameters $\{\alpha_1, \alpha_2\}$. Both auxiliary parameters are outside the unit circle when the algorithms converge to the region with two degrees of indeterminacy. Across all simulations, when starting from one of the alternative regions, the auxiliary parameters $\{\alpha_1, \alpha_2\}$ eventually jump and after that they never take values within the unit circle again. In Section 6, we use the model of Lubik and Schorfheide (2004) to show that when the determinate and indeterminate regions of the parameter space present a more similar fit, the hybrid algorithm facilitates the transition between them. We show that when using the hybrid algorithm, the auxiliary parameter frequently jumps between values within and outside of the unit circle, carrying valuable information about the probability attached to determinacy and ensuring a faster convergence with respect to the traditional random walk algorithm.

¹³In Appendix B, Table 5 reports the Raftery-Lewis diagnostics for each parameter chain in Galí (forthcoming). Using the hybrid algorithm, all the model parameters quickly converge.

Parameter estimates and impulse responses. Table 2 also reports the mean and 90% probability interval of the posterior distribution of the estimated structural parameters. The posterior mean of the slope of the NK Phillips curve is 0.038, which in this model is consistent with a probability of roughly 25% that a firm keeps its price unchanged in any given period. The steady-state quarterly growth rate of output, g , is about 0.48% and the resulting real interest rate, r , is 0.44%. The posterior mean for the inflation rate, π^* , is about 3.6% on an annual basis. The strength of the responses of U.S. monetary policy to inflation and the bubble was not enough to guarantee a stabilization of the U.S. economy and to avoid that unexpected changes in expectations could drive U.S. business cycles. The posterior mean of the term λ_l is 0.9997 such that probability of remaining “active” is $v = \lambda_l \beta / \Lambda \Gamma = 0.997$.

The mean of the standard error of the bubble component is 1.19, and larger than that of the supply and monetary policy shocks estimated to be 0.11 and 0.12, respectively. The data also provide evidence that the bubble shock is nearly as persistent as the supply shock. The posterior estimate of the standard error related to forecast errors for the output gap is roughly twice as large as that of the sunspot shock associated with the inflation rate. As discussed next, the estimates of the correlations between the sunspot and exogenous shocks of the model and those between the two sunspot shocks are crucial to interpret the contemporaneous impact of each shock and the associated impulse responses.

Figure 2 plots the impulse response functions of output, inflation, the FFR, and the Real FFR to a one-standard-deviation fundamental and sunspot shocks.¹⁴ The solid lines represent the posterior median, while the dark and light shaded areas correspond to the 68% and 90% probability intervals respectively. In line with the estimated correlations reported in Table 2, we observe that a shock due to the creation of a new bubble generates a positive contemporaneous and persistent effect on inflation. Moreover, the value of asset bubbles is higher over time due to its increasing expected value. The monetary authority responds to these deviations by increasing the nominal FFR, causing a slight slowdown in economic activity over the period shown. The estimated correlations of the supply shock with the sunspot shocks induce both an inflationary and contractionary effects on impact. The persistence of the shock on output is then associated to deflationary effects to which the monetary authority responds by decreasing the FFR.

As indicated in Table 2, a monetary policy shock is negatively correlated with both sunspot shocks, implying a negative contemporaneous impact on both inflation and output. The contemporaneous effect of the shock on the FFR combines the downward impact on both inflation and the bubble component with the upward effect of the monetary policy shock itself. The initial positive monetary policy shock is almost perfectly offset by the endogenous component, with the result that the nominal FFR remains close to zero despite the initial shock. However, the Real

¹⁴The real FFR corresponds to the difference between the FFR and the one-period ahead inflation expectation.

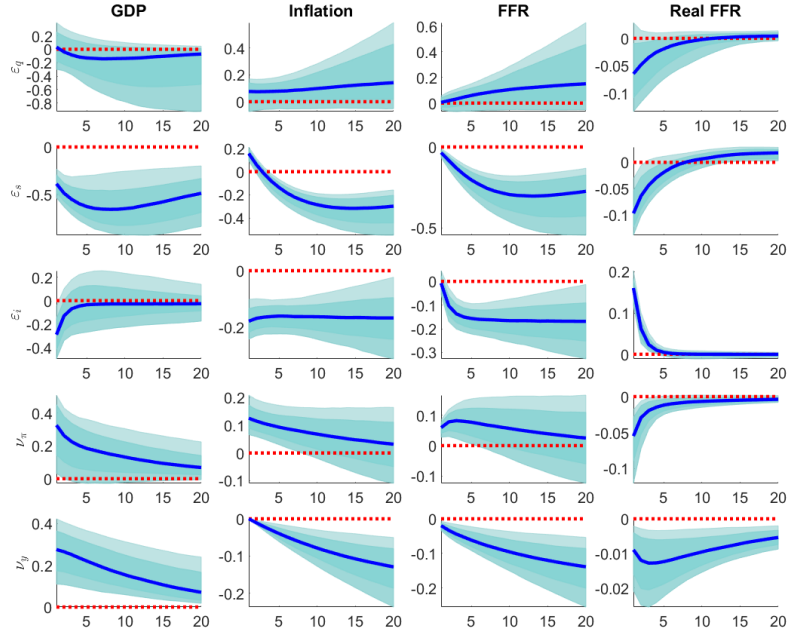


Figure 2: Bayesian impulse response functions.

Each panel plots the posterior mean (solid lines), the 68-percent probability interval (dark blue, shaded) and 90-percent probability interval (light blue, shaded) for the impulse responses of output, inflation and Federal Funds rate (FFR) to a shock of one standard deviation for each orthogonalized disturbance using a Cholesky decomposition with the same order as in the figure.

FFR still increases in response to the positive monetary policy shock, as illustrated in the last column of Figure 2. Thus, a positive monetary policy shock is still contractionary despite the equilibrium behavior of the nominal FFR. The rise in the Real FFR combined with the decrease in expectations about the future value of the bubble generates a downward contemporaneous impact on the value of the asset today (equation (11) in the model). The persistence of these effects on the real economy and the inflation rate requires the monetary authority to adopt an accommodative stance. The behavior of the nominal FFR is reminiscent of an example presented in Galí (2008) in the context of a prototypical purely forward-looking three-equation NK model. Galí (2008) shows that if a monetary policy shock has very large effects on the macroeconomy, the monetary policy interest rate can decline in equilibrium, despite the monetary policy shock being positive.

The last two panels show the impulse responses to the sunspot shocks, that we assume to be uncorrelated with each other. A positive shock to inflation expectations, ν_π , generates a contemporaneous rise in inflation. The Real FFR decreases due to an increase of inflation expectations

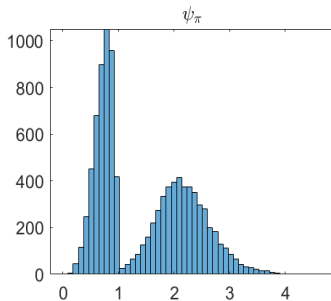


Figure 3: Posterior distribution of ψ_π in Lubik and Schorfheide (2004).

The figure reports the posterior distribution of the parameter ψ_π when using the hybrid algorithm.

that more than compensates for the rise in the FFR. The drop in the Real FFR and higher expectations about the future value of the bubble explain the rise in economic activity and a higher current value of the bubble, consistent with a more restrictive monetary policy stance. Finally, a positive sunspot shock to output expectations leads to a rise in economic activity. Such increase is consistent with higher aggregate fundamental wealth in the economy and a lower current and expected value of the bubble.¹⁵ Given that the Cholesky decomposition assumes that the output sunspot shock, ν_y , is orthogonal to the inflation sunspot shock, ν_π , a one-standard deviation shock to ν_y has no contemporaneous effect on inflation, while it generates mild deflationary effects in the medium term due to a decrease in inflation expectations. On impact, monetary policy responds to the decrease in the current value of the asset bubble and subsequently adopts a more accommodative stance also induced by the deflationary pressure.

6 Advantages of the hybrid algorithm

In this section, we discuss the advantages of using the hybrid estimation algorithm for the case in which the fit of the model at the global peak is only marginally better than that at a local peak belonging to a different region of indeterminacy. To provide an example of this case, we estimate the three-equation NK model in Lubik and Schorfheide (2004) over the “Post-1982” period using our solution method and hybrid algorithm.¹⁶ The parameter space is characterized by a region of determinacy and a region of indeterminacy of degree 1. To solve the model under indeterminacy, we augment it by appending only one auxiliary process. The global peak in the determinate region marginally outperforms the local peak in the region of one-degree indeterminacy. Based

¹⁵The model in Galí (forthcoming) includes the equation $y_t = (1 - \beta\nu)(q_t + x_t)$, where x_t denotes aggregate fundamental wealth (i.e. discounted sum of current and future income expected to accrue to currently alive consumers) normalized by trend output.

¹⁶We refer the reader to Lubik and Schorfheide (2004) for a detailed description of the standard model.

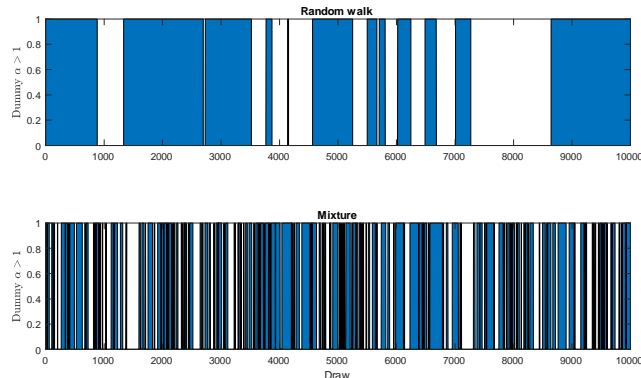


Figure 4: Jumps between determinacy and indeterminacy in Lubik and Schorfheide (2004).

The figure reports the draws of the parameters θ in the determinate and indeterminate region using the random walk (panel above) and hybrid (panel below) algorithms. A dummy variable has a value of 1 for each draw of parameters in the determinate region ($\alpha > 1$) and a value of 0 for draws in the indeterminate region ($\alpha \leq 1$). The blue/dark area plots values of the dummy equal to 1, while the white area plots values equal to 0.

on the marginal data density under determinacy (-236.81) and indeterminacy (-236.84), the resulting posterior probability of determinacy is 50.5% based on the modified harmonic mean estimator of Geweke (1999a).

When estimating the model in Lubik and Schorfheide (2004) using the Mixture algorithm, Figure 3 plots the resulting bimodal distribution of the parameter ψ_π that governs the response of the monetary authority to deviations of the inflation rate from its target.

To cautiously verify the converge of the model parameters, we assign a value of 1 to a dummy variable for each draw of structural parameters in the determinate region ($\alpha > 1$) and a value of 0 for draws in the indeterminate region ($\alpha \leq 1$). Figure 4 reports values of the dummy equal to 1 (blue/dark areas) and evidently shows that, while both algorithms visit the two regions, the Mixture algorithm jumps between them much more frequently ensuring an efficient exploration of the parameter space. In particular, using the hybrid algorithm, the parameter α is greater than 1 in 51.45% of the accepted draws, therefore containing relevant information related to the probability of determinacy. Finally, in Appendix C, Table 6 reports the Raftery-Lewis diagnostics for each parameter using the two algorithms: The Mixture algorithm cuts the number of draws required for convergence in half.¹⁷

¹⁷We target the 5% quantile, with 1% precision, and 90% probability.

7 Conclusions

In this paper, we propose a generalized approach to solve and estimate LRE models over the entire parameter space. Our approach accommodates both cases of determinacy and indeterminacy and it does not require the researcher to know the analytic conditions describing the region of determinacy or the degrees of indeterminacy.

When a LRE model is characterized by m degrees of indeterminacy, our approach appends m autoregressive processes whose innovations are linear combinations of a subset of endogenous shocks and a vector of newly defined sunspot shocks. We show that the solution for the resulting augmented representation embeds both the solution which is obtained under determinacy using standard solution methods and that delivered by solving the model under indeterminacy using the approach of Lubik and Schorfheide (2003) and equivalently Farmer et al. (2015).

We pair our solution method with an hybrid MCMC algorithm to estimate the small-scale NK model of Galí (forthcoming). Galí's model extends a conventional NK model by allowing for the existence of rational bubbles and is characterized by up to two degrees of indeterminacy for realistic parameter values. We estimate the model using U.S. data over the period 1982:Q4-2007:Q3. We find that the data support the version of the model with two degrees of indeterminacy, implying that the central bank was not reacting strongly enough to the bubble component. Finally, we show that our MCMC hybrid algorithm facilitates the transition to the correct area of the posterior and repeated jumps between local peaks of the posterior when these are close in value. Relative to the standard random walk Metropolis-Hastings algorithm, the hybrid algorithm minimizes the possibility of remaining stuck in an area of the posterior characterized by a local peak and substantially improves the speed of convergence.

References

- S. Adjemian, H. Bastani, M. Juillard, J. Maih, F. Karamé, F. Mihoubi, G. Perendia, J. Pfeifer, M. Ratto, and S. Villemot. Dynare: Reference manual version 4. *Dynare Working Papers, CEPREMAP*, 1, 2011.
- S. An and F. Schorfheide. Bayesian analysis of dsge models. *Econometric Reviews*, 26(2–4): 113–172, 2007.
- J. E. Arias, G. Ascari, N. Branzoli, and E. Castelnuovo. Positive trend inflation and determinacy in a medium-sized new keynesian model. *International Journal of Central Banking*, forthcoming.
- S. B. Aruoba, P. Cuba-Borda, and F. Schorfheide. Macroeconomic Dynamics Near the ZLB: A Tale of Two Countries. *Review of Economic Studies*, 85:87–118, 2018.
- G. Ascari, P. Bonomolo, and H. F. Lopes. Walk on the wild side: Temporarily unstable paths and multiplicative sunspots. *The American Economic Review*, 109(5):1805–42, 2019.
- O. J. Blanchard and C. M. Kahn. The solution of linear difference models under rational expectations. *Econometrica*, 48:1305–1313, 1980.
- D. Cass and K. Shell. Do sunspots matter? *Journal of Political Economy*, 91:193–227, 1983.
- L. Christiano, M. Eichenbaum, and C. Evans. Nominal rigidities and the dynamics effects of a shock to monetary policy. *Journal of Political Economy*, 113:1–45, 2005.
- R. Clarida, J. Galí, and M. Gertler. Monetary policy rules and macroeconomic stability: Evidence and some theory. *Quarterly Journal of Economics*, CXV:147–180, 2000.
- O. Coibon and Y. Gorodnichenko. Monetary policy, trend inflation, and the Great Moderation: An Alternative Interpretation. *American Economic Review*, 101(1):341–370, 2011.
- S. Ettmeier and A. Kriwoluzky. Active, or Passive? Revisiting the Role of Fiscal Policy in the Great Inflation. DIW Belin, Discussion Papers, 2020.
- R. E. Farmer, V. Khramov, and G. Nicolò. Solving and Estimating Indeterminate DSGE Models. *Journal of Economic Dynamics and Control*, 54:17–36, 2015.
- R. E. A. Farmer and J. T. Guo. Real business cycles and the animal spirits hypothesis. *Journal of Economic Theory*, 63:42–73, 1994.

- R. E. A. Farmer and J.-T. Guo. The econometrics of indeterminacy. *Carnegie Rochester Series on Public Policy*, 43:225–273, 1995.
- J. Galí. *Monetary Policy, Inflation, and the Business Cycle: An Introduction to the New Keynesian Framework*. Princeton University Press, 2008.
- J. Galí. Monetary Policy and Bubbles in a New Keynesian Model with Overlapping Generations. *American Economic Journal: Macroeconomics*, forthcoming.
- J. Geweke. Using simulation methods for bayesian econometric models: Inference, development, and communication. *Econometric Reviews*, 18:1–73, 1999a.
- J. Geweke. Using simulation methods for bayesian econometric models: Inference, development, and communication. *Econometric Reviews*, 18(1):1–73, 1999b.
- P. Giordani, R. Kohn, and I. Strid. Adaptive hybrid Metropolis-Hastings samplers for DSGE models. *SSE/EFI Working Paper Series in Economics and Finance*, 724(February), 2010.
- E. P. Herbst and F. Schorfheide. *Bayesian Estimation of DSGE Models*. Princeton University Press, 2015a.
- E. P. Herbst and F. Schorfheide. Sequential Monte Carlo Sampling for DSGE Models. *Journal of Applied Econometrics*, 45(4):693–705, 2015b.
- Y. Hirose, T. Kurozumi, and W. V. Zandweghe. Monetary Policy and Macroeconomic Stability Revisited. *Review of Economic Dynamics*, 37, 2020.
- W. R. Kerr and R. G. King. Limits on interest rate rules in is-lm models. *Federal Reserve Bank of Richmond Economic Quarterly*, 82(2):47–75, 1996.
- R. G. King and M. Watson. The solution of singular linear difference systems under rational expectations. *International Economic Review*, 39(4):1015–1026, 1998.
- P. Klein. Using the generalized schur form to solve a multivariate linear rational expectations model. *Journal of Economic Dynamics and Control*, 24(10):1405–1423, 2000.
- T. A. Lubik and F. Schorfheide. Computing sunspot equilibria in linear rational expectations models. *Journal of Economic Dynamics and Control*, 28(2):273–285, 2003.
- T. A. Lubik and F. Schorfheide. Testing for indeterminacy: An application to U.S. monetary policy. *American Economic Review*, 94:190–219, 2004.
- C. A. Sims. Solving linear rational expectations models. *Journal of Computational Economics*, 20(1-2):1–20, 2001.

8 Appendix

8.1 Appendix A

8.1.1 Equivalence under determinacy

This section considers the case in which the original LRE is determinate, and shows the equivalence of the solution obtained using the proposed augmented representation with the one from the standard solution method described in Sims (2001).

Canonical solution Consider the LRE model in (5) and reported in the following equation

$$\underset{k \times k}{\Gamma_0} \underset{k \times 1}{X_t} = \underset{k \times k}{\Gamma_1} \underset{k \times 1}{X_{t-1}} + \underset{k \times l}{\Psi} \underset{l \times 1}{\varepsilon_t} + \underset{k \times p}{\Pi} \underset{p \times 1}{\eta_t}. \quad (15)$$

The method described in Sims (2001) delivers a solution, if it exists, by following four steps. First, Sims (2001) shows how to write the model in the form

$$SZ'X_t = TZ'X_{t-1} + Q\Psi\varepsilon_t + Q\Pi\eta_t, \quad (16)$$

where $\Gamma_0 = Q'SZ'$ and $\Gamma_1 = Q'TZ'$ result from the QZ decomposition of $\{\Gamma_0, \Gamma_1\}$, and the $k \times k$ matrices Q and Z are orthonormal, upper triangular and possibly complex. Also, the diagonal elements of S and T contain the generalized eigenvalues of $\{\Gamma_0, \Gamma_1\}$.

Second, given that the QZ decomposition is not unique, Sims' algorithm chooses a decomposition that orders the equations so that the absolute values of the ratios of the generalized eigenvalues are placed in an increasing order, that is

$$|t_{jj}|/|s_{jj}| \geq |t_{ii}|/|s_{ii}| \quad \text{for } j > i.$$

The algorithm then partitions the matrices S , T , Q and Z as

$$S = \begin{bmatrix} S_{11} & S_{12} \\ 0 & S_{22} \end{bmatrix}, \quad T = \begin{bmatrix} T_{11} & T_{12} \\ 0 & T_{22} \end{bmatrix}, \quad Z' = \begin{bmatrix} Z_1 \\ Z_2 \end{bmatrix}, \quad Q = \begin{bmatrix} Q_1 \\ Q_2 \end{bmatrix},$$

where the first block corresponds to the system of equations for which $|t_{jj}|/|s_{jj}| \leq 1$ and the second block groups the equations which are characterized by explosive roots, $|t_{jj}|/|s_{jj}| > 1$.

The third step imposes conditions on the second, explosive block to guarantee the existence of

at least one bounded solution. Defining the transformed variables

$$\xi_t \equiv Z' X_t = \begin{bmatrix} \xi_{1,t} \\ (k-n) \times 1 \\ \xi_{2,t} \\ n \times 1 \end{bmatrix},$$

where n is the number of explosive roots, and the transformed parameters

$$\tilde{\Psi} \equiv Q' \Psi, \quad \text{and} \quad \tilde{\Pi} \equiv Q' \Pi,$$

the second block can be written as

$$\xi_{2,t} = S_{22}^{-1} T_{22} \xi_{2,t-1} + S_{22}^{-1} (\tilde{\Psi}_2 \varepsilon_t + \tilde{\Pi}_2 \eta_t).$$

As this system of equations contains the explosive roots of the original system, then a bounded solution, if it exists, will set

$$\xi_{2,0} = 0 \tag{17}$$

$$\tilde{\Psi}_2 \varepsilon_t + \tilde{\Pi}_2 \eta_t = 0, \tag{18}$$

where n also denotes the number of equations in (18). A necessary condition for the existence of a solution requires that the number of unstable roots (n) equals the number of expectational variables (p). In this section, we are considering the solution under determinacy, and this guarantees that there are no degrees of indeterminacy $m^*(\theta) = 0$. The sufficient condition then requires that the columns of the matrix $\tilde{\Pi}_2$ are linearly independent so that there is at least one bounded solution. In that case, the matrix $\tilde{\Pi}_2$ is a square, non-singular matrix and equation (18) imposes linear restrictions on the forecast errors, η_t , as a function of the fundamental shocks, ε_t ,

$$\eta_t = -\tilde{\Pi}_2^{-1} \tilde{\Psi}_2 \varepsilon_t. \tag{19}$$

The fourth and last step finds the solution for the endogenous variables, X_t , by combining the restrictions in (17) and (19) with the system of stable equations in the first block,

$$\begin{aligned} \xi_{1,t} &= S_{11}^{-1} T_{11} \xi_{1,t-1} + S_{11}^{-1} (\tilde{\Psi}_1 \varepsilon_t + \tilde{\Pi}_1 \eta_t) \\ &= S_{11}^{-1} T_{11} \xi_{1,t-1} + S_{11}^{-1} \left(\tilde{\Psi}_1 - \tilde{\Pi}_1 \tilde{\Pi}_2^{-1} \tilde{\Psi}_2 \right) \varepsilon_t \end{aligned} \tag{20}$$

Using the algorithm by Sims (2001), we can describe the solution under determinacy of the LRE model in (15) with equations (17), (19), and (20).

Augmented representation We now consider the methodology proposed in this paper, and we augment the LRE model in (15) with the following system of m equations

$$\omega_t = \Phi\omega_{t-1} + \nu_t - \eta_{f,t}, \quad \Phi \equiv \begin{bmatrix} \frac{1}{\alpha_1} & & \mathbf{0} \\ & \ddots & \\ \mathbf{0} & & \frac{1}{\alpha_m} \end{bmatrix}$$

where Φ is a $m \times m$ diagonal matrix. As the original model in (15) is determinate, then we assume that all the diagonal elements α_i belong to the interval $[1, 2]$. Therefore, we are appending a system of stable equations, and we show that the solution for the endogenous variables, X_t , is equivalent to the one found in Subsection 8.1.1. Defining the augmented vector of endogenous variables, $\hat{X}_t \equiv (X_t, \omega_t)'$ and the augmented vector of exogenous shocks $\hat{\varepsilon}_t \equiv (\varepsilon_t, \nu_t)'$, the representation that we propose takes the form

$$\hat{\Gamma}_0 \hat{X}_t = \hat{\Gamma}_1 \hat{X}_{t-1} + \hat{\Psi} \hat{\varepsilon}_t + \hat{\Pi} \eta_t, \quad (21)$$

where

$$\hat{\Gamma}_0 \equiv \begin{bmatrix} \Gamma_0 & \mathbf{0} \\ \mathbf{0} & \mathbf{I} \end{bmatrix}, \quad \hat{\Gamma}_1 \equiv \begin{bmatrix} \Gamma_1 & \mathbf{0} \\ \mathbf{0} & \Phi \end{bmatrix}, \quad \hat{\Psi} \equiv \begin{bmatrix} \Psi & \mathbf{0} \\ \mathbf{0} & \mathbf{I} \end{bmatrix}, \quad \hat{\Pi} \equiv \begin{bmatrix} \Pi_n & \Pi_f \\ 0 & -\mathbf{I} \end{bmatrix},$$

and without loss of generality the matrix Π is partitioned as $\Pi = [\Pi_n \quad \Pi_f]$, where the matrices Π_n and Π_f are respectively of dimension $k \times (p - m)$ and $k \times m$.

We can find a solution to the augmented representation in (21) by using Sims' algorithm. Similarly to the previous section, we follow the four steps which describe the algorithm. First, the solution algorithm performs the QZ decomposition of the matrices $\{\hat{\Gamma}_0, \hat{\Gamma}_1\}$ and the augmented representation takes the form

$$\hat{S} \hat{Z}' \hat{X}_t = \hat{T} \hat{Z}' \hat{X}_{t-1} + \hat{Q} \hat{\Psi} \hat{\varepsilon}_t + \hat{Q} \hat{\Pi} \eta_t, \quad (22)$$

where $\hat{\Gamma}_0 = \hat{Q}' \hat{S} \hat{Z}'$ and $\hat{\Gamma}_1 = \hat{Q}' \hat{T} \hat{Z}'$ result from the QZ decomposition of $\{\hat{\Gamma}_0, \hat{\Gamma}_1\}$, and

$$\hat{S} = \begin{bmatrix} S_{11} & \mathbf{0} & S_{12} \\ \mathbf{0} & \mathbf{I} & \mathbf{0} \\ \mathbf{0} & \mathbf{0} & S_{22} \end{bmatrix}, \quad \hat{T} = \begin{bmatrix} T_{11} & \mathbf{0} & T_{12} \\ \mathbf{0} & \Phi & \mathbf{0} \\ \mathbf{0} & \mathbf{0} & T_{22} \end{bmatrix}, \quad \hat{Z}' = \begin{bmatrix} Z_1 & \mathbf{0} \\ \mathbf{0} & \mathbf{I} \\ Z_2 & \mathbf{0} \end{bmatrix}, \quad \hat{Q} = \begin{bmatrix} Q_1 & \mathbf{0} \\ \mathbf{0} & \mathbf{I} \\ Q_2 & \mathbf{0} \end{bmatrix}.$$

Importantly, note that the inner matrices of $\{\hat{S}, \hat{T}, \hat{Z}, \hat{Q}\}$ are the same as those which define the matrices $\{S, T, Z, Q\}$ found in the previous section using the canonical solution method.

Second, the algorithm chooses a QZ decomposition which groups the equations in a stable and an explosive block. Because this section assumes that the original model is determinate and that the diagonal elements of the matrix Φ are within the unit circle, the explosive block corresponds to the third system of equations in (22) which is characterized by explosive roots. Recalling the definition of the matrices $\hat{\Psi}$ and $\hat{\Pi}$, the system of equations in the third block is

$$\xi_{2,t} = S_{22}^{-1}T_{22}\xi_{2,t-1} + S_{22}^{-1}(\tilde{\Psi}_2\varepsilon_t + \tilde{\Pi}_2\eta_t). \quad (23)$$

The third step imposes conditions to guarantee the existence of a bounded solution. However, the explosive block in (23) is identical to the system of equations found in the previous section. Therefore, the algorithm imposes the same restrictions to guarantee the existence of a bounded solution, that is

$$\xi_{2,0} = 0 \quad (24)$$

and as found earlier

$$\eta_t = -\tilde{\Pi}_2^{-1}\tilde{\Psi}_2\varepsilon_t. \quad (25)$$

Finally, the last step combines these restrictions with the system of equations in the stable block which corresponds to the first and second systems of equations in (22),

$$\xi_{1,t} = S_{11}^{-1}T_{11}\xi_{1,t-1} + S_{11}^{-1}\left(\tilde{\Psi}_1 - \tilde{\Pi}_1\tilde{\Pi}_2^{-1}\tilde{\Psi}_2\right)\varepsilon_t, \quad (26)$$

$$\omega_t = \Phi\omega_{t-1} + \nu_t - \eta_{f,t}. \quad (27)$$

Recalling that $\xi_t \equiv Z'X_t$, the solution in (24)~(27) obtained for the augmented representation of the LRE model delivers the same solution for the endogenous variables of interest, X_t , found in the previous section and defined in equations (17), (19), and (20).

8.1.2 Equivalence under indeterminacy

This section shows the equivalence of the solutions obtained for a LRE model under indeterminacy using the proposed augmented representation and the methodology of Lubik and Schorfheide (2003, 2004).

Lubik and Schorfheide (2003) As in Subsection 8.1.1, we consider the LRE model in (15) and reported below as (28)

$$\Gamma_0 X_t = \Gamma_1 X_{t-1} + \Psi\varepsilon_t + \Pi\eta_t. \quad (28)$$

In this section we assume that the model is indeterminate, and we present the method used by Lubik and Schorfheide (2003). The authors implement the first two steps of the algorithm by Sims (2001) and described in Subsection 8.1.1.¹⁸ They proceed by first applying the QZ decomposition to the LRE model in (28) and then ordering the resulting system of equations in a stable and an explosive block as defined in equation (16). However, their approach differs in the third step when the algorithm imposes restrictions to guarantee the existence of a bounded solution. In particular, the restrictions in (17) and (18) reported below as (29) and (30) require that

$$\xi_{2,0} = 0, \quad (29)$$

$$\tilde{\Psi}_2 \varepsilon_t + \tilde{\Pi}_2 \eta_t = 0. \quad (30)$$

Nevertheless, it is clear that the system of equation in (30) is indeterminate as the number of forecast errors exceeds the number of explosive roots ($p > n$). Equivalently, there are less equations (n) than the number of variables to solve for (p). To characterize the full set of solutions to equation (30), Lubik and Schorfheide (2003) decompose the matrix $\tilde{\Pi}_2$ using the following singular value decomposition

$$\tilde{\Pi}_2 \equiv U \begin{bmatrix} D_{11} & \mathbf{0} \\ & \end{bmatrix} V',$$

where m represents the degrees of indeterminacy. Given the partition $V \equiv \begin{bmatrix} V_1 & V_2 \\ & \end{bmatrix}$, equation (30) can be written as

$$D_{11}^{-1} U' \tilde{\Psi}_2 \varepsilon_t + V_1' \eta_t = 0. \quad (31)$$

Given that the system is indeterminate, Lubik and Schorfheide (2003) append additional m equations,

$$\tilde{M} \varepsilon_t + M_\zeta \zeta_t = V_2' \eta_t. \quad (32)$$

The $m \times 1$ vector ζ_t is a set of sunspot shocks that is assumed to have mean zero, covariance matrix $\Omega_{\zeta\zeta}$ and to be uncorrelated with the fundamental shocks, ε_t , that is

$$E[\zeta_t] = 0, \quad E[\zeta_t \varepsilon_t'] = 0, \quad E[\zeta_t \zeta_t'] = \Omega_{\zeta\zeta}.$$

¹⁸It is relevant to mention that in this section the matrices obtained from the QZ decomposition and the ordering of the equations into a stable and an explosive block differ from those in Subsection 8.1.1 both in terms of their dimensionality and the elements constituting them. However, we opted to use the same notation for simplicity.

The matrix \widetilde{M} captures the correlation of the forecast errors, η_t , with fundamentals, ε_t , and Lubik and Schorfheide (2003) choose the normalization $M_\zeta = I_m$. The reason to append the system of equations in (32) to the equations in (31) is to exploit the properties of the orthonormal matrix V . Premultiplying the system by the matrix V and recalling that $V * V' = I$, the expectational errors can be written as a function of the fundamental shocks, ε_t , and the sunspot shocks, ζ_t ,

$$\eta_t = \begin{pmatrix} -V_1 D_{11}^{-1} U_1' \widetilde{\Psi}_2 + V_2 \widetilde{M} \\ \end{pmatrix} \begin{matrix} \varepsilon_t \\ \zeta_t \end{matrix}.$$

More compactly,

$$\eta_t = \begin{pmatrix} V_1 N + V_2 \widetilde{M} \\ \end{pmatrix} \begin{matrix} \varepsilon_t \\ \zeta_t \end{matrix}, \quad (33)$$

where

$$N \equiv -D_{11}^{-1} U_1' \widetilde{\Psi}_2.$$

is a function of the parameters of the model. Given the restriction in (29) and (33), the fourth step in the algorithm combines these equations with the system of stable equations in the first block as in Subsection 8.1.1,

$$\begin{aligned} \xi_{1,t} &= S_{11}^{-1} T_{11} \xi_{1,t-1} + S_{11}^{-1} (\widetilde{\Psi}_1 \varepsilon_t + \widetilde{\Pi}_1 \eta_t) \\ &= S_{11}^{-1} T_{11} \xi_{1,t-1} + S_{11}^{-1} \left(\widetilde{\Psi}_1 + \widetilde{\Pi}_1 V_1 N + \widetilde{\Pi}_1 V_2 \widetilde{M} \right) \varepsilon_t + S_{11}^{-1} \left(\widetilde{\Pi}_1 V_2 \right) \zeta_t. \end{aligned} \quad (34)$$

Using the method in Lubik and Schorfheide (2003), we can describe the solution for the original LRE model under indeterminacy with equations (29), (33) and (34).

Augmented representation We now consider the augmented representation as in (21) and reported below as

$$\widehat{\Gamma}_0 \widehat{X}_t = \widehat{\Gamma}_1 \widehat{X}_{t-1} + \widehat{\Psi} \widehat{\varepsilon}_t + \widehat{\Pi} \eta_t, \quad (35)$$

where $\widehat{X}_t \equiv (X_t, \omega_t)'$, $\widehat{\varepsilon}_t \equiv (\varepsilon_t, \nu_t)'$ and

$$\widehat{\Gamma}_0 \equiv \begin{bmatrix} \Gamma_0 & \mathbf{0} \\ \mathbf{0} & \mathbf{I} \end{bmatrix}, \quad \widehat{\Gamma}_1 \equiv \begin{bmatrix} \Gamma_1 & \mathbf{0} \\ \mathbf{0} & \Phi \end{bmatrix}, \quad \widehat{\Psi} \equiv \begin{bmatrix} \Psi & \mathbf{0} \\ \mathbf{0} & \mathbf{I} \end{bmatrix}, \quad \widehat{\Pi} \equiv \begin{bmatrix} \Pi_n & \Pi_f \\ 0 & -\mathbf{I} \end{bmatrix}.$$

where the matrix Π is partitioned as $\Pi = [\Pi_n \quad \Pi_f]$ without loss of generality.

The novelty of our approach is that, given our representation, we can easily obtain the solution by using Sims' algorithm even when the original LRE is assumed to be indeterminate. It is enough to assume that the auxiliary processes ω_t are characterized by explosive roots, or equivalently that the diagonal elements of the matrix Φ are outside the unit circle. This approach guarantees

that the Blanchard-Kahn condition for the augmented representation is satisfied and, given the analytic form that we propose for the auxiliary processes, we show that the solution for the endogenous variables of interest, X_t , is equivalent to the method of Lubik and Schorfheide (2003).

To show this result, we simply apply the four steps of the algorithm described in Sims (2001) to the proposed augmented representation. First, the QZ decomposition of (35) takes the form

$$\hat{S}\hat{Z}'\hat{X}_t = \hat{T}\hat{Z}'\hat{X}_{t-1} + \hat{Q}\hat{\Psi}\hat{\varepsilon}_t + \hat{Q}\hat{\Pi}\eta_t, \quad (36)$$

where $\hat{\Gamma}_0 = \hat{Q}'\hat{S}\hat{Z}'$ and $\hat{\Gamma}_1 = \hat{Q}'\hat{T}\hat{Z}'$ result from the QZ decomposition¹⁹ of $\{\hat{\Gamma}_0, \hat{\Gamma}_1\}$ and

$$\hat{S} = \begin{bmatrix} S_{11} & S_{12} & \mathbf{0} \\ \mathbf{0} & S_{22} & \mathbf{0} \\ \mathbf{0} & \mathbf{0} & \mathbf{I} \end{bmatrix}, \quad \hat{T} = \begin{bmatrix} T_{11} & T_{12} & \mathbf{0} \\ \mathbf{0} & T_{22} & \mathbf{0} \\ \mathbf{0} & \mathbf{0} & \Phi \end{bmatrix}, \quad \hat{Z}^T = \begin{bmatrix} Z_1 & \mathbf{0} \\ Z_2 & \mathbf{0} \\ \mathbf{0} & \mathbf{I} \end{bmatrix}, \quad \hat{Q} = \begin{bmatrix} Q_1 & \mathbf{0} \\ Q_2 & \mathbf{0} \\ \mathbf{0} & \mathbf{I} \end{bmatrix}. \quad (37)$$

Note that in the expression above the auxiliary matrix Φ is in the lower (explosive) block because of our simplifying assumption that $m^*(\theta) = m$. When $m^*(\theta) < m$, part of the matrix Φ would belong in the stable block. As mentioned above, we made this simplifying assumption without loss of generality and only to simplify the exposition.

Second, the QZ decomposition chosen by the algorithm groups the explosive dynamics of the model in the second and third system of equations in (36), which are reported below as (38)

$$\begin{bmatrix} S_{22} & \mathbf{0} \\ \mathbf{0} & \mathbf{I} \end{bmatrix} \begin{bmatrix} \xi_2 \\ \omega_t \end{bmatrix} = \begin{bmatrix} T_{22} & \mathbf{0} \\ \mathbf{0} & \Phi \end{bmatrix} \begin{bmatrix} \xi_{2,t-1} \\ \omega_{t-1} \end{bmatrix} + \begin{bmatrix} Q_2 & \mathbf{0} \\ \mathbf{0} & \mathbf{I} \end{bmatrix} (\hat{\Psi}\hat{\varepsilon}_t + \hat{\Pi}\eta_t). \quad (38)$$

In the third step, the following restrictions are imposed,

$$\xi_{2,0} = 0, \quad (39)$$

$$\omega_0 = 0, \quad (40)$$

$$\begin{bmatrix} Q_2 & \mathbf{0} \\ \mathbf{0} & \mathbf{I} \end{bmatrix} (\hat{\Psi}\hat{\varepsilon}_t + \hat{\Pi}\eta_t) = 0. \quad (41)$$

¹⁹Note that the inner matrices of $\{\hat{S}, \hat{T}, \hat{Z}^T, \hat{Q}\}$ are the same as those which define the matrices $\{S, T, Z^T, Q\}$ found from the QZ decomposition using the methodology of Lubik and Schorfheide (2003).

Recalling the definition of $\hat{\Psi}$ and $\hat{\Pi}$ in (35), then equation (41) can be written as

$$\underbrace{\begin{bmatrix} \tilde{\Psi}_2 & \mathbf{0} \\ \mathbf{0} & \mathbf{I} \end{bmatrix}}_{p \times (\ell+m)} \hat{\varepsilon}_t + \underbrace{\begin{bmatrix} \tilde{\Pi}_{n,2} & \tilde{\Pi}_{f,2} \\ \mathbf{0} & -\mathbf{I} \end{bmatrix}}_{p \times p} \eta_t = 0, \quad (42)$$

where $\tilde{\Psi} \equiv Q'\Psi$ and $\tilde{\Pi} \equiv Q'\Pi$. Equation (42) shows transparently how the explosive auxiliary process that we append in our augmented representation helps to solve the original LRE model under indeterminacy. The system of equations in (42) is determinate, as the number of equations defined by the explosive roots of the system equals the number of expectational errors of the model. Thus, the necessary condition for the existence of a bounded solution for the augmented representation is satisfied. Assuming that the columns of the matrix associated with the vector of non-fundamental shocks, η_t , are linearly independent, we can impose linear restrictions on the forecast errors as a function of the augmented vector of exogenous shocks $\hat{\varepsilon}_t \equiv (\varepsilon_t, \nu_t)'$,

$$\eta_t = - \begin{bmatrix} \tilde{\Pi}_{n,2}^{-1} \tilde{\Psi}_2 & \tilde{\Pi}_{n,2}^{-1} \tilde{\Pi}_{f,2} \\ \mathbf{0} & -\mathbf{I} \end{bmatrix} \hat{\varepsilon}_t.$$

More compactly,

$$\eta_t = C_1 \varepsilon_t + C_2 \nu_t, \quad (43)$$

where $C_1 \equiv - \begin{bmatrix} \tilde{\Pi}_{n,2}^{-1} \tilde{\Psi}_2 \\ \mathbf{0} \end{bmatrix}$ and $C_2 \equiv - \begin{bmatrix} \tilde{\Pi}_{n,2}^{-1} \tilde{\Pi}_{f,2} \\ -\mathbf{I} \end{bmatrix}$ are a function of the structural parameters of the model.

The last step of Sims' algorithm combines the restrictions in (39), (40) and (43) with the stationary block derived from the QZ decomposition in (36),

$$\begin{aligned} \xi_{1,t} &= S_{11}^{-1} T_{11} \xi_{1,t-1} + S_{11}^{-1} (\tilde{\Psi}_1 \varepsilon_t + \tilde{\Pi}_1 \eta_t) \\ &= S_{11}^{-1} T_{11} \xi_{1,t-1} + S_{11}^{-1} (\tilde{\Psi}_1 + \tilde{\Pi}_1 C_1) \varepsilon_t + S_{11}^{-1} (\tilde{\Pi}_1 C_2) \nu_t. \end{aligned} \quad (44)$$

8.1.3 Mapping of normalization in Lubik and Schorfheide (2004) to Bianchi-Nicolò

We prove the equivalence between the parametrization of the Lubik-Schorfheide indeterminate equilibrium $\theta^{LS} \in \Theta^{LS}$ and the Bianchi-Nicolò equilibrium parametrized by $\theta^{BN} \in \Theta^{BN}$. In particular, we show that there is a unique mapping between the linear restrictions imposed in each of the two methodologies on the forecast errors to guarantee the existence of at least a bounded solution. As shown in Subsection 8.1.2, the method by Lubik and Schorfheide (2003) imposes the following restrictions on the non-fundamental shocks, η_t , as a function of the exogenous shocks,

ε_t , and the sunspot shocks introduced in their specification, ζ_t ,

$$\eta_t = \begin{pmatrix} V_1 N + V_2 \widetilde{M} \\ p \times n \times \ell \quad p \times m \times \ell \\ m \times \ell \end{pmatrix} \varepsilon_t + V_2 \zeta_t. \quad (45)$$

Using the methodology proposed in this paper, Subsection 8.1.2 shows that the restrictions on the non-fundamental shocks, η_t , as a function of the exogenous shocks, ε_t , and the sunspot shocks, ν_t , are

$$\eta_t = C_1 \varepsilon_t + C_2 \nu_t, \quad (46)$$

where

$$C_1 \equiv - \begin{bmatrix} \widetilde{\Pi}_{n,2}^{-1} \widetilde{\Psi}_2 \\ \mathbf{0} \end{bmatrix} \quad \text{and} \quad C_2 \equiv - \begin{bmatrix} \widetilde{\Pi}_{n,2}^{-1} \widetilde{\Pi}_{f,2} \\ -\mathbf{I} \end{bmatrix}.$$

Post-multiplying equation (45) and (46) by ε_t' and taking expectations on both sides,

$$\begin{aligned} \Omega_{\eta\varepsilon} &= V_1 N \Omega_{\varepsilon\varepsilon} + V_2 \widetilde{M} \Omega_{\varepsilon\varepsilon}, \\ \Omega_{\eta\varepsilon} &= C_1 \Omega_{\varepsilon\varepsilon} + C_2 \Omega_{\nu\varepsilon} \end{aligned}$$

Pre-multiplying by V_2' and equating the equations,

$$\widetilde{M} \Omega_{\varepsilon\varepsilon} = \begin{pmatrix} V_2' C_1 - V_2' V_1 N \\ m \times p \quad p \times \ell \quad m \times p \quad p \times n \times \ell \end{pmatrix} \Omega_{\varepsilon\varepsilon} + V_2' C_2 \Omega_{\nu\varepsilon}. \quad (47)$$

Using the properties of the *vec* operator, the following result holds

$$\text{vec}(\widetilde{M}) = \begin{pmatrix} \Omega_{\varepsilon\varepsilon} \otimes I_m \\ (m \times \ell) \times 1 \quad (m \times \ell) \times (m \times \ell) \end{pmatrix}^{-1} \begin{bmatrix} [I_l \otimes (V_2' C_1 - V_2' V_1 N)] \text{vec}(\Omega_{\varepsilon\varepsilon}) + (I_l \otimes V_2' C_2) \text{vec}(\Omega_{\nu\varepsilon}) \\ (m \times \ell) \times \ell^2 \quad \ell^2 \times 1 \quad (m \times \ell) \times (m \times \ell) \quad (m \times \ell) \times 1 \end{bmatrix}. \quad (48)$$

Equation (48) is the first relevant equation to show the mapping between the representation in Lubik and Schorfheide (2003) and our representation. For a given variance-covariance matrix of the exogenous shocks, $\Omega_{\varepsilon\varepsilon}$, that is common between the two representations, equation (48) tells us that the covariance structure, $\Omega_{\nu\varepsilon}$, of the sunspot shock in our representation with the exogenous shocks has a unique mapping to the matrix, \widetilde{M} , in Lubik and Schorfheide (2003). Clearly, equation (47) can also be used to derive the mapping from their representation to our method.

We now show how to derive the mapping between the variance-covariance matrix, $\Omega_{\nu\nu}$, of the sunspot shocks in our representation to the variance-covariance matrix, $\Omega_{\zeta\zeta}$, of the sunspot shocks

in Lubik and Schorfheide (2003). Considering again equation (45) and (46), we post-multiply by ζ'_t and take expectations on both sides,

$$\begin{aligned}\Omega_{\eta\zeta} &= V_2 \Omega_{\zeta\zeta}, \\ \Omega_{\eta\zeta} &= C_2 \Omega_{\nu\zeta}\end{aligned}$$

Pre-multiplying both equations by V_2' and equating them,

$$\Omega_{\zeta\zeta} = \Omega_{\zeta\nu} (V_2' C_2)'. \quad (49)$$

Finally, to obtain an expression for $\Omega_{\zeta\nu}$, we post-multiply equation (45) and (46) by ν'_t and taking expectations

$$\begin{aligned}\Omega_{\eta\nu} &= \left(V_1 N + V_2 \widetilde{M} \right) \Omega_{\varepsilon\nu} + V_2 \Omega_{\zeta\nu}, \\ \Omega_{\eta\nu} &= C_1 \Omega_{\varepsilon\nu} + C_2 \Omega_{\nu\nu}\end{aligned}$$

Pre-multiplying both equations by V_2' and solving for $\Omega_{\zeta\nu}$,

$$\Omega_{\zeta\nu} = \left(V_2' C_1 - V_2' V_1 N - \widetilde{M} \right) \Omega_{\varepsilon\nu} + (V_2' C_2) \Omega_{\nu\nu}. \quad (50)$$

Post-multiplying (50) by $(V_2' C_2)'$ and using (49), then

$$\Omega_{\zeta\zeta} = \left(V_2' C_1 - V_2' V_1 N - \widetilde{M} \right) \Omega_{\varepsilon\nu} (V_2' C_2)' + (V_2' C_2) \Omega_{\nu\nu} (V_2' C_2)'. \quad (51)$$

Therefore, equation (51) defines the mapping between the variance-covariance matrix, $\Omega_{\nu\nu}$, of the sunspot shocks in our representation to the variance-covariance matrix, $\Omega_{\zeta\zeta}$, of the sunspot shocks in Lubik and Schorfheide (2003). Together with equation (48), we show that this equation defines the one-to-one mapping between the parametrization in Lubik and Schorfheide $\{\Theta, \Theta^{LS}\}$ and the parametrization in Bianchi-Nicolò $\{\Theta, \Theta^{BN}\}$.

8.2 Appendix B

Table 4 reports the posterior distribution of the model parameters for each of the three specifications that are possible when adopting our method to solve for the model of Galí (forthcoming) under two degrees of indeterminacy. For each specification, the log-posterior mode is -33.1 and the table shows that the estimates are equivalent up to a transformation of the correlations between the exogenous shocks and the forecast errors included in the auxiliary process.²⁰

	$\{\nu_1=\nu_\pi, \nu_2 = \nu_y\}$		$\{\nu_1=\nu_\pi, \nu_2 = \nu_b\}$		$\{\nu_1=\nu_y, \nu_2 = \nu_b\}$	
	Mean	90% prob. int.	Mean	90% prob. int.	Mean	90% prob. int.
$100(\lambda_l^{-1}-1)$	0.028	[0.018,0.038]	0.031	[0.018,0.043]	0.030	[0.012,0.042]
κ	0.042	[0.034,0.050]	0.039	[0.031,0.047]	0.039	[0.031,0.047]
g	0.48	[0.46,0.50]	0.49	[0.46,0.51]	0.48	[0.46,0.51]
π^*	0.89	[0.44,1.36]	0.90	[0.41,1.36]	0.89	[0.40,1.34]
ϕ_π	0.29	[0.14,0.43]	0.34	[0.15,0.56]	0.26	[0.12,0.39]
ϕ_q	0.02	[0.01,0.04]	0.04	[0.01,0.07]	0.03	[0.01,0.04]
ρ_i	0.50	[0.27,0.74]	0.50	[0.25,0.77]	0.48	[0.23,0.73]
σ_q	0.97	[0.45,1.51]	1.21	[0.45,2.06]	1.01	[0.46,1.58]
σ_s	0.11	[0.09,0.12]	0.11	[0.09,0.14]	0.11	[0.09,0.13]
σ_i	0.11	[0.09,0.14]	0.12	[0.09,0.15]	0.12	[0.09,0.14]
ρ_q	0.71	[0.55,0.87]	0.74	[0.57,0.91]	0.72	[0.56,0.87]
ρ_s	0.89	[0.84,0.94]	0.88	[0.81,0.95]	0.88	[0.83,0.94]
σ_{ν_1}	0.30	[0.25,0.34]	0.30	[0.25,0.34]	0.70	[0.61,0.79]
σ_{ν_2}	11.14	[5.48,16.55]	0.71	[0.61,0.80]	10.10	[4.83,15.39]
$\varphi_{\nu_1,i}$	-0.54	[-0.75,-0.31]	-0.59	[-0.80,-0.39]	-0.38	[-0.65,-0.11]
$\varphi_{\nu_1,q}$	0.18	[-0.27,0.60]	0.21	[-0.23,0.62]	0.11	[-0.43,0.66]
$\varphi_{\nu_1,s}$	0.58	[0.46,0.72]	0.54	[0.38,-0.69]	-0.54	[-0.70,-0.40]
$\varphi_{\nu_2,i}$	-0.72	[-0.88,-0.54]	-0.39	[-0.71,-0.10]	-0.76	[-0.93,-0.61]
$\varphi_{\nu_2,q}$	-0.06	[-0.42,0.29]	0.05	[-0.44,0.56]	-0.08	[-0.46,0.26]
$\varphi_{\nu_2,s}$	-0.51	[-0.71,-0.32]	-0.55	[-0.72,-0.38]	-0.45	[-0.65,-0.25]
φ_{ν_1,ν_2}	0.28	[0.03,0.54]	0.23	[0.05,0.41]	0.63	[0.44,0.81]

Table 4: Posterior distribution of model parameters under 2-degree indeterminacy.

Below, Table 5 reports the Raftery-Lewis diagnostics for each parameter chain of the model of Galí (forthcoming).

²⁰To obtain the estimates in Table 4, we use a uniform distribution over the interval (0,20) for the standard deviation of the sunspot shocks. This guarantees that the posterior distribution of the sunspot shock ν_b is not at the boundary of the range specified for the uniform prior.

Variable	Thin	Burn	Total (N)	Nmin	I-stat
$100(\lambda_l^{-1} - 1)$	1	2	345	322	1.071
κ	1	2	304	322	0.944
g	1	2	331	322	1.028
π^*	1	3	293	322	0.910
ϕ_π	1	2	304	322	0.944
ϕ_q	1	2	317	322	0.984
ρ_i	1	3	361	322	1.121
σ_q	1	2	331	322	1.028
σ_s	1	3	376	322	1.168
σ_i	1	2	345	322	1.071
ρ_q	1	3	376	322	1.168
ρ_s	1	2	331	322	1.028
σ_{ν_π}	1	3	340	322	1.056
σ_{ν_y}	1	2	345	322	1.071
$\varphi_{\nu_\pi, i}$	1	3	392	322	1.217
$\varphi_{\nu_\pi, q}$	1	3	376	322	1.168
$\varphi_{\nu_\pi, s}$	1	4	410	322	1.273
$\varphi_{\nu_y, i}$	1	3	376	322	1.168
$\varphi_{\nu_y, q}$	1	4	410	322	1.273
$\varphi_{\nu_y, s}$	1	3	385	322	1.196
φ_{ν_π, ν_y}	1	13	985	322	3.059

Table 5: Raftery-Lewis Diagnostics for each parameter chain in Galí (forthcoming).

The table reports the Raftery-Lewis diagnostics for each parameter chain. We consider the 5th quantile, $q = 0.05$, with an accuracy $r = 0.02$ and a probability $s = 0.9$ of obtaining an estimate in the interval $(q - r, q + r)$. The diagnostics reports the suggested number of burn-in iterations ("Burn"), the suggested number of iterations ("Total (N)"), the suggested minimum number of iterations based on zero autocorrelation ("Nmin") and the dependence factor ("I-stat"). The dependence factor is computed as $\text{I-stat} = (\text{Burn} + \text{Total})/\text{Nmin}$, and interpreted as the proportional increase in the number of iterations attributable to autocorrelation.

8.3 Appendix C

	Mixture					Random walk				
	Thin	Burn	Total (N)	Nmin	I-stat	Thin	Burn	Total (N)	Nmin	I-stat
ψ_π	2	5	2981	1286	2.318	4	14	5790	1286	4.502
ψ_y	1	2	1299	1286	1.010	1	1	1287	1286	1.000
ρ_R	1	3	1545	1286	1.201	1	3	1432	1286	1.113
τ	1	3	1564	1286	1.216	1	3	1538	1286	1.196
κ	2	7	3037	1286	2.362	1	4	1654	1286	1.286
ρ_g	2	7	2967	1286	2.307	4	15	6287	1286	4.889
ρ_z	1	2	1332	1286	1.036	1	2	1321	1286	1.027
r^*	1	3	1468	1286	1.141	1	3	1474	1286	1.146
π^*	1	3	1500	1286	1.166	3	11	4136	1286	3.216
σ_R	1	2	1366	1286	1.062	1	3	1526	1286	1.187
σ_g	1	2	1372	1286	1.067	1	3	1384	1286	1.076
σ_z	1	2	1304	1286	1.014	1	1	1285	1286	0.999
ρ_{gz}	2	7	3051	1286	2.372	2	8	2972	1286	2.311
σ_η	2	6	2758	1286	2.145	1	3	1390	1286	1.081

Table 6: Raftery-Lewis Diagnostics for each parameter chain in Lubik and Schorfheide (2004).

The table reports the Raftery-Lewis diagnostics for each parameter chain using the hybrid ("Mixture") and the random walk algorithm ("Random walk"). We consider the 5th quantile, $q = 0.05$, with an accuracy $r = 0.01$ and a probability $s = 0.9$ of obtaining an estimate in the interval $(q - r, q + r)$. The diagnostics reports the suggested number of burn-in iterations ("Burn"), the suggested number of iterations ("Total (N)"), the suggested minimum number of iterations based on zero autocorrelation ("Nmin") and the dependence factor ("I-stat"). The dependence factor is computed as $\text{I-stat} = (\text{Burn} + \text{Total})/\text{Nmin}$, and interpreted as the proportional increase in the number of iterations attributable to autocorrelation.

8.4 Appendix D

In this section, we consider the case that a researcher estimates a LRE model using Bayesian techniques and a conventional Metropolis-Hastings algorithm in Dynare. Let us consider the following LRE model

$$\Gamma_0(\theta)X_t = \Gamma_1(\theta)X_{t-1} + \Psi(\theta)\varepsilon_t + \Pi(\theta)\eta_t, \quad (52)$$

with a maximum degree of indeterminacy denoted by m .²¹ As explained in detail in Section 3, the proposed methodology appends to the original LRE model the following system of m equations

$$\omega_t = \Phi\omega_{t-1} + \nu_t - \eta_{f,t}, \quad (53)$$

where Φ is a diagonal matrix whose entries are $\{1/\alpha_1, \dots, 1/\alpha_m\}$. Denoting the newly defined vector of endogenous variables $\hat{X}_t \equiv (X_t, \omega_t)'$ and the newly defined vector of exogenous shocks $\hat{\varepsilon}_t \equiv (\varepsilon_t, \nu_t)'$, the resulting augmented LRE model can be written as

$$\hat{\Gamma}_0\hat{X}_t = \hat{\Gamma}_1\hat{X}_{t-1} + \hat{\Psi}\hat{\varepsilon}_t + \hat{\Pi}\eta_t. \quad (54)$$

Auxiliary autoregressive parameters. As a first step, we discuss how to handle the vector of additional autoregressive parameters, $\{\alpha_i\}_{i=1}^m$, introduced under our methodology. We can distinguish three cases:

1. When the threshold for the different regions of determinacy is known analytically, then α_i can be expressed as a function of the other parameters. In this case, there is no need to specify a prior on α_i and the prior probability of (in)determinacy is given by the prior on the parameter vector θ .
2. When the threshold is unknown and the researcher writes her own code, she can start with all the roots inside the unit circle for α at each draw of θ and then flip the appropriate number of elements in the vector α . This case coincides with the approach that we adopt in Section 5 to estimate the model of Galí (forthcoming) for which there is no need to specify a prior on α_i and the prior probability of indeterminacy depends on the prior on the parameter vector θ . In other words, in this case α_i is treated as an unknown transformation of the structural parameters that guarantees that a solution, if it exists, can be found independently of the degree of indeterminacy.
3. When the threshold is unknown and the researcher wants to use standard estimation packages such as Dynare, there are two options. First, the researcher estimates the model

²¹We refer the reader to Section 3 for definitions and notation.

separately for different degrees of indeterminacy. This is the simplest approach and we describe it more in detail below. Second, the researcher estimates the model over the whole parameter space. In this case, the researcher can complement the Dynare codes with a function that pins down the degrees of indeterminacy. This can be done writing a function that, starting with all $\{\alpha_i\}_{i=1}^m$ inside the unit circle, solves the model and keeps flipping $\{\alpha_i\}_{i=1}^m$ until the augmented state space returns determinacy. In this case, the $\{\alpha_i\}_{i=1}^m$ are still treated as a transformation of the structural parameters of the model. Alternatively, the researcher can decide to treat $\{\alpha_i\}_{i=1}^m$ as additional parameters. In this case, the researcher should choose priors that are symmetric with respect to the various determinacy regions and orthogonal with respect to the priors on the other parameters. The researcher could use a uniform distribution over the interval $[0.5, 1.5]$ or any symmetric interval around 1 as a prior distribution. The assumptions that the priors are symmetric around 1 and orthogonal with respect to the structural parameters imply that the a-priori probabilities of the different determinacy regions only depend on the priors on the structural parameters of the model. The posterior distribution of the parameters is not affected by treating $\{\alpha_i\}_{i=1}^m$ as additional parameters. However, the priors on $\{\alpha_i\}_{i=1}^m$ would have an impact on the marginal data density computed by Dynare. The marginal data density can be corrected ex-post by taking into account that uniform priors on $\{\alpha_i\}_{i=1}^m$ simply rescale the joint prior on the model parameters. Alternatively, a researcher could implement a simple modification of the code used to compute Geweke (1999)’s modified harmonic mean estimator to remove the impact of the priors on α_i . For example, $\{\alpha_i\}_{i=1}^m$ could be weighted using their own prior when computing the modified harmonic mean estimator.

Priors for the correlations between the sunspot and fundamental shocks. In Subsection 2.2, we discuss in detail the economic rationale for how to construct a baseline solution using our methodology. Therefore, it seems natural to center the prior distribution for the correlations on zero, the value associated with the “baseline solution.” However, as carefully explained in Subsection 2.2, it is important to stress that under the baseline solution, the choice of which forecast errors to include in the auxiliary processes matters for the solution when the correlations are restricted to zero. At the same time, as explained in Section 3, a set of correlations under the representation that includes a given subset of non-fundamental shocks has a unique mapping to *different* values of the correlations in the representation with another subset of non-fundamental disturbances, and vice versa. Therefore, in order for the alternative representations to deliver the same fit to the data, a researcher has to leave the *correlations unrestricted*. One simple option is to set a uniform prior distributions over the interval $(-1, 1)$ for the correlations of the sunspot shocks. As shown for the estimation of the model of Galí (forthcoming) in Section 5, this approach guarantees that the fit of the model does not depend on which non-fundamental

shock is included in the auxiliary processes. Of course, if a researcher has reasons to believe that one baseline solution is more meaningful than the other, she can choose the priors accordingly. Lubik and Schorfheide (2004) center the prior distribution for the additional parameters introduced in their representation to values that minimize the distance between the impulse responses of the model under indeterminacy and determinacy evaluated at the boundary of the region of determinacy. While our approach and intuition differ, our theoretical results show the equivalence between the two representations in Section 3. Therefore, the priors for the correlations between sunspot shocks and fundamental shocks could also be specified in a way to replicate the approach of Lubik and Schorfheide (2004). Specifically, we could center the prior on the auxiliary parameters as in Lubik and Schorfheide (2004) and then map those values into correlations in our approach that would deliver the same fit of the model to the data. However, our suggestion to choose a flat prior such as a uniform distribution considers a-priori the mapped parameterization suggested by Lubik and Schorfheide (2004) as equally likely with respect to the continuum of indeterminate equilibria.

Model comparison. A researcher might be interested in comparing the fit of the model under determinacy and under indeterminacy. Note that, while under indeterminacy the volatility of the sunspot shocks and their correlations with the exogenous shocks are estimated, those parameters *should* be restricted to zero (or any other constant) under determinacy. Model comparison can then be conducted by using standard techniques, such as the harmonic mean estimator proposed by Geweke (1999b).